AD-A051 398 NAVAL ELECTRONICS LAB CENTER SAN DIEGO CALIF F/G 9/5
SOME ELECTRICAL AND OPERATING CHARACTERISTICS OF INTEGRATED POW--ETC(U)
MAR 68 S E PARKER, J M DEVAN, W J EDWARDS

UNCLASSIFIED NELC-1551 NL

| OF |
AD
A051 398

END
DATE
FILMED
4-78
DDC

END
DATE
FILMED
4-78
DDC

SOME ELECTRICAL AND OPERATING CHARACTERISTICS OF INTEGRATED POWER AMPLIFIER COUPLER EQUIPMENT

Empirical evaluation shows that the performance characteristics are in substantial agreement with theoretical predictions

S. E. Parker, J. M. Devan, W. J. E. Edwards, and L. G. Robbins

Research and Development Report **18 March 1968**

NAVAL ELECTRONICS LABORATORY CENTER
San Diego, California 92152

PROBLEM

Perform an empirical evaluation of the efficiency, stability, attenuation, and cross-modulation characteristics of high-power hf power amplifier coupler (PAC) equipment to expedite an objective comparison with conventional multicoupling techniques.

RESULTS

1. An evaluation of integrated PAC equipment showed that:

a. Its essential performance characteristics are in substantial agreement with predictions based on analytical studies.

b. Compared with a transmitter and a two-mesh coupler, the integrated three-mesh assembly affords increased selectivity urgently needed in alleviating interference aboard ships from their own high-power hf transmitters.

c. As presently designed, the experimental PAC equipment provides operation that is electrically and operationally stable at the 10 kilowatt (PEP) plate-power level.

2. Auxiliary tests in this program did not support the theory that magnetic material used in Type UG-30 D/U and UG-30 E/U feedthrough connectors is itself a significant source of nonlinear products, even at extreme power levels for fittings of this type. Since these spurious signals can originate from dirty, corroded, and poorly made connections, however, cable fittings should be of high quality and kept to a practical minimum.

RECOMMENDATIONS

1. Procure sufficient PAC and bandpass distribution line (D-line) equipment to facilitate a full-scale testing and evaluation program in a simulated shipboard installation.

2. In the meantime, perform analyses and tests to more completely delineate the capabilities and limitations of the modular bandpass D-line. In addition to single coupler groups, this investigation should include the use of two complementary D-lines with a common antenna load (both real and simulated).

3. Extend the integrated PAC concept to radio receiving systems.

4. Conduct design studies, as required, to facilitate the integration of transmitting and receiving couplers with a common antenna. This capability is especially needed with directional broadband antennas such as log-periodic structures.

5. Perform analytical and empirical studies to permit realistic predictions of cross-modulation products generated in representative power amplifier tubes, taking into account forward and reverse characteristics of PAC equipment.

ADMINISTRATIVE INFORMATION

This work was performed under S32-78, Task 7398 (NELC J543) by a special task group in the Electromagnetics Technology Department. The authors were assisted by G. E. Bartz, P. A. Jensen, H. J. Jourdan, and other Laboratory personnel too numerous to mention. The work was done between January and September 1967, and the report was approved for publication 18 March 1968.

CONTENTS

ILLUSTRATIONS

Illustrations (Continued)

Illustrations (Continued)

TABLES

Tables (Continued)

INTRODUCTION

In October 1966 comparative tests were undertaken involving alternative transmitting multicoupling approaches being considered under the Naval Ships Advanced Communication System (NSACS) project. These tests were intended to assist in preparing specifications for ultra-reliable hf radio equipment for ships such as the Numbered Fleet Flagship (NFF) having major command and control functions

Because of limited time and manpower, testing had to be restricted to the efficiency, stability and selectivity characteristics of the coupling networks. Studies involving the capabilities and limitations of alternative combining or distribution schemes were not included.

Two small task groups investigated the two alternative approaches under consideration. One group tested AN/SRA-35(V)(XN-2) multicoupling equipment with two AN/FRT-39A radio transmitters; the other tested integrated power amplifier coupler (PAC) equipment.

DESCRIPTION OF EQUIPMENT UNDER TEST

Equipment tested in the PAC phase of the evaluation (fig. 1) included two PAC assemblies (seen in the foreground) interconnected by a bandpass distribution line (D-line). Two AN/FRT-39A radio transmitters are shown in the background.

Figure 2 shows one of the experimental PAC assemblies with certain panels removed to illustrate components and other details. Modular construction permits different power amplifier units to be used. Also, by removing the central resonator, the number of meshes in the coupler assembly can be reduced from three to two. This particular D-line can accommodate as many as six PAC assemblies.

A typical resonator unit (fig. 3) contains a large inductor made of silver-plated copper tubing. The inductor is cradled by three supports fabricated of grooved sheets of Teflon that are supported in turn by sheets of silicone fiber glass and special brass brackets (as shown at left in the sketch). The inductor is connected in series with a Jennings ceramic vacuum variable capacitor. Ground connections are made at top and bottom of the enclosure. Resonators of this general design have satisfactorily passed shock and vibration requirements of MIL-E-16400E.

Each resonator is cooled by air and water. A blower mounted below each enclosure supplies 140 cubic feet of air per minute. Tap water is circulated at a rate of about 2 gallons per minute through the large inductor by means of a 3/8-inch plastic tube within the large copper tube. A small coil of 1/4-inch copper tubing carries circulating water to the stationary plate assembly of the capacitor. The main inductors were originally fabricated of flattened copper tubing soldered together, as shown in figure 2, but the use of plastic inner tubing affords significant savings and, it now appears, will give long, trouble-free service.

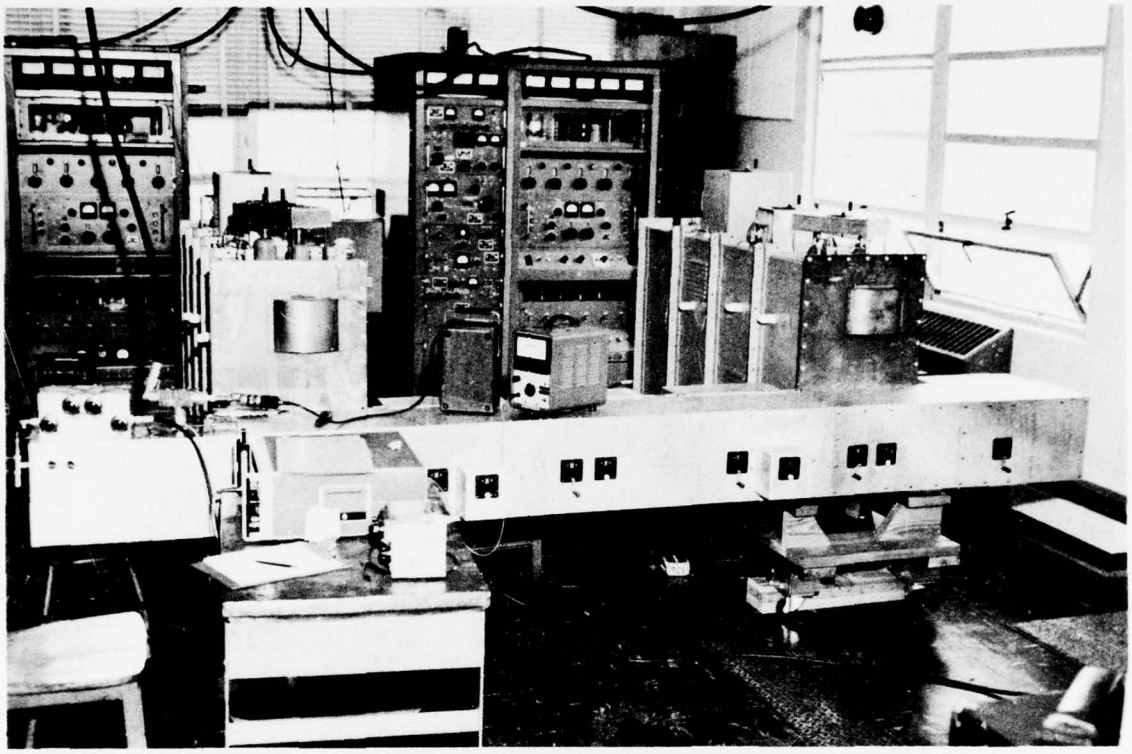

Figure 1. Photograph of PAC equipment tested.

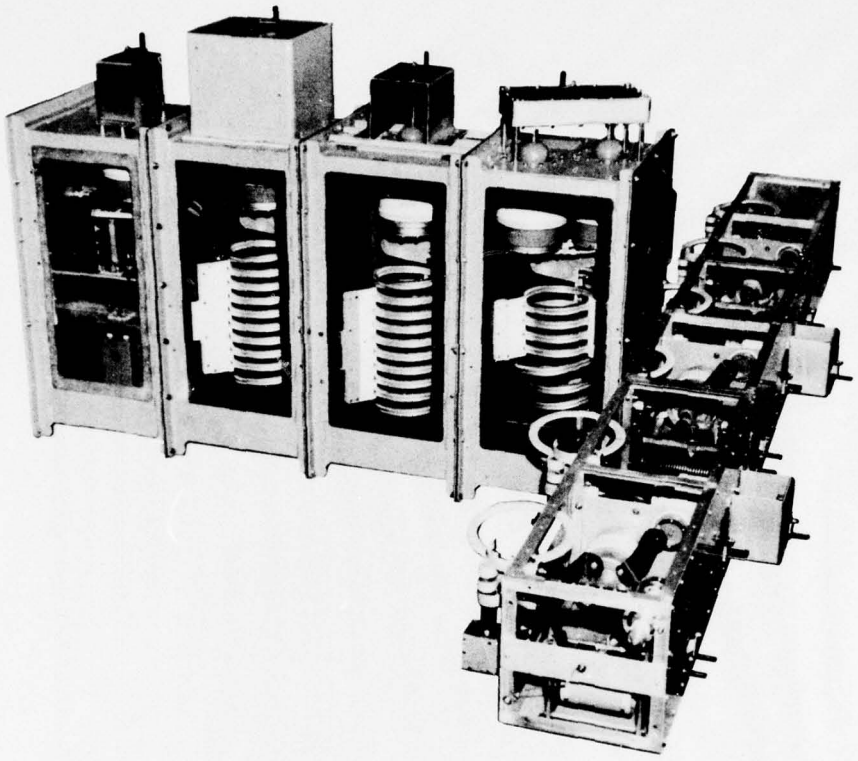

Figure 2. Photograph of experimental PAC and D-line equipment with side-panels and cover-plates removed.

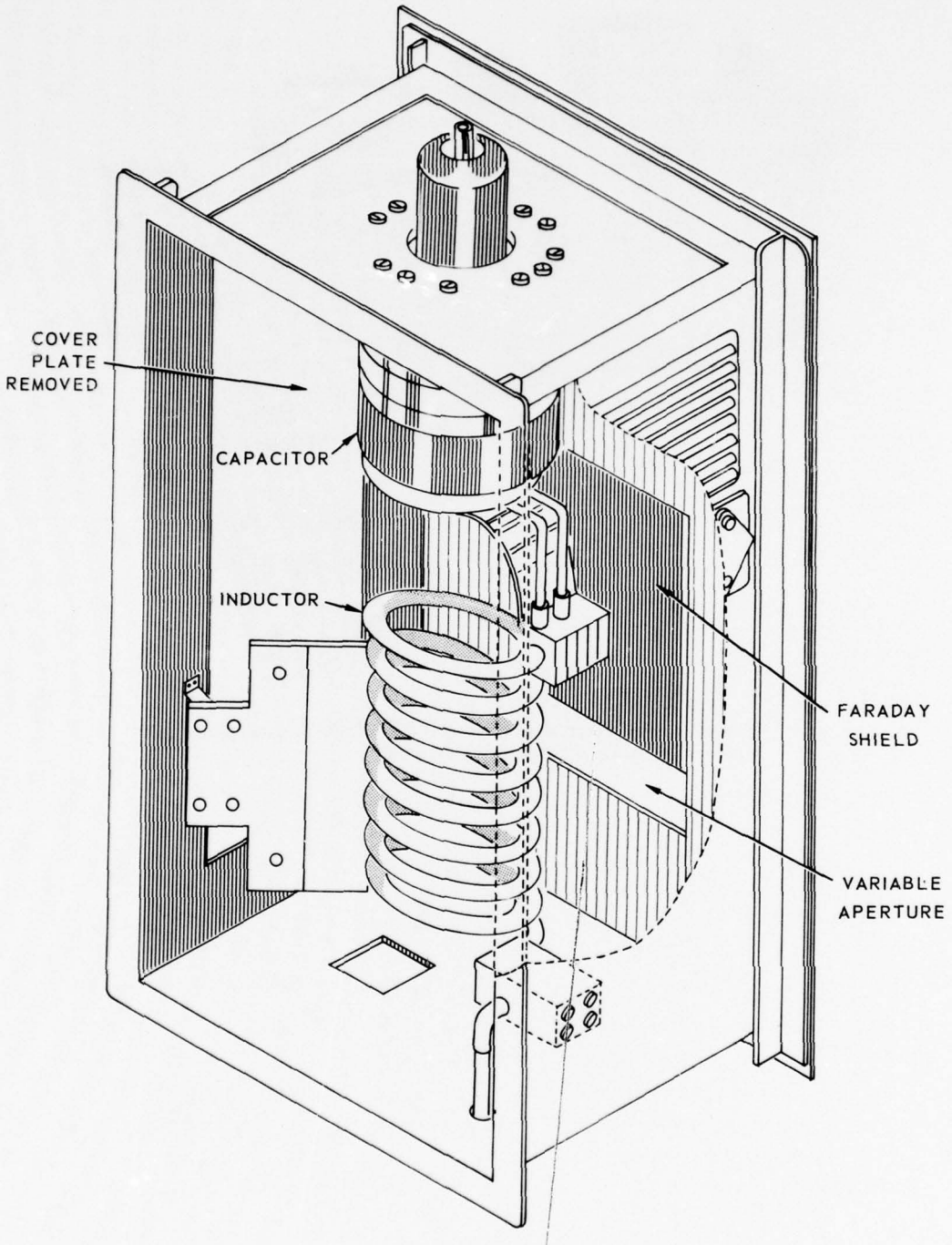

Figure 3. Typical resonator unit in a PAC assembly.

Experimental equipment used in this study was designed to utilize certain commercial units already installed in the NELC Transmitter Laboratory. For early tests at moderate power level, excitation was obtained from an AN/URC-32B radio set. For testing at nominal 5-kilowatt power levels, a 4CX5000A beam tetrode was used in each power amplifier module. Since the same tube is used in each of the two AN/FRT-39A radio transmitters in the Laboratory, excitation, as well as proper polarizing potentials, for operating the PAC equipment was obtained by relatively simple interconnections with the AN/FRT-39A transmitters. This arrangement also afforded essential safety measures, permitting interlocks on the PAC units to be connected with the interlock circuits of the commercial transmitters.

A complete schematic diagram of a 5-kilowatt PAC assembly is shown in figure 4. A special *L*-type matching network is used to provide a nominal 50-ohm load for the intermediate power amplifier stage (IPA) of the AN/FRT-39A transmitter. While the metering circuits were not changed, the bypassing scheme originally used with the 4CX5000A tube was modified by adding a 0.02 μF capacitor between screen and ground and a 1000 pF capacitor from grid to ground. This additional bypassing reduced the amount of negative feedback employed in the commercial transmitters but significantly improved the stability of the power amplifier. (A tendency toward parasitic oscillations was particularly troublesome during initial cross-modulation tests.)

The distribution line is a form of bandpass structure that has been described in an earlier report.[1] Design details and performance characteristics of this distribution technique are not within the scope of this study. It is sufficient for present purposes to note that the structure in figure 2 will accommodate as many as six separate PAC assemblies with a common load. It is designed for a nominal 50-ohm impedance level with the geometric mean frequency of its passband being set at 2.828 MHz. (This early experimental structure was subsequently redesigned to form, in effect, an essentially 50-ohm rectangular "trunk," thus minimizing effects of lead inductance between the six coupling links.)

---

[1]Superscript numbers denote references at end of report.

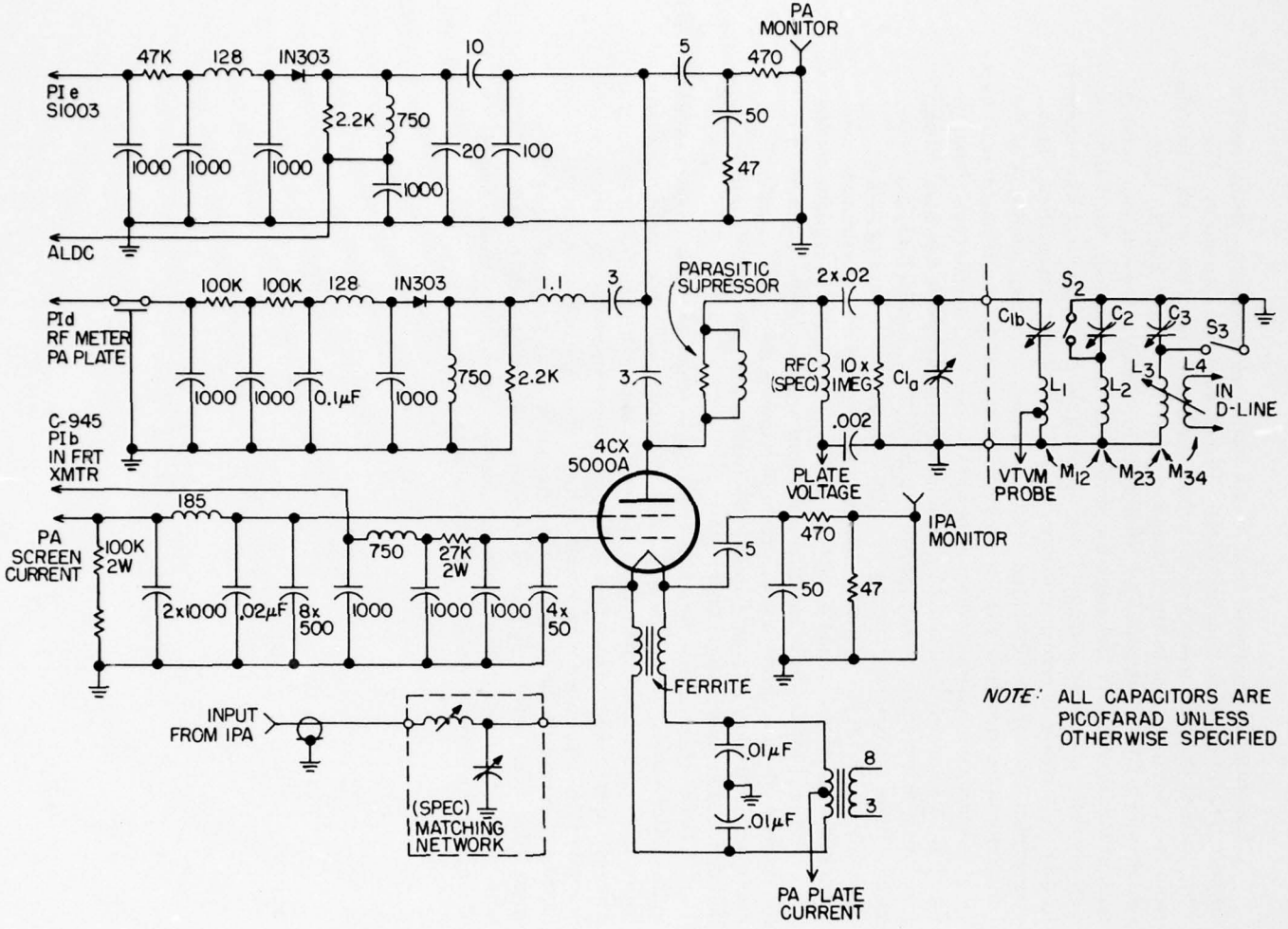

Figure 4. Complete schematic diagram of three-mesh 5-kilowatt PAC assembly.

ADJUSTMENT AND OPERATING PROCEDURE

The procedure used in tuning and loading the meshes of a PAC assembly was that of Dishal,[2] modified by an important final step. Beginning with the output mesh, each resonator was tuned and loaded in turn to reduce the unloaded Q by a factor of 7. Having pre-established the desired positions of the adjustable apertures in this manner, a VTVM (loosely coupled L_1) was used as an indicator as the following steps were performed in succession:

1. C_{1a} was tuned for maximum deflection of the VTVM with vacuum relay S_2 closed,

2. C_2 was tuned for VTVM minimum with S_2 opened and S_3 closed,

3. C_3 was tuned for VTVM maximum with S_2 and S_3 opened (and the output coupling set for proper 7-to-1 loading of the output mesh, as explained above); and finally

4. C_{1a} was readjusted to provide a purely resistive load at the plates of the power tubes, as indicated by minimum plate current.

The capacitor C_{1b} in figure 4 was preset to give the proper value of the plate load resistance at each frequency.

To obtain an indication of the precision of adjustment obtained by the modified Dishal procedure outlined above, the input impedance of a three-mesh coupling network was measured at frequencies extending some 5 percent above and below the operating frequency f_0 at the low end, the middle, and the high end of the operating band. As shown in figures 5 through 10, these measured data compare favorably with input resistance and reactance obtained by digital computer, using measured values of network components and resonator Q-factors. The data in figures 5 and 6 apply to the low end of the band, the data in figures 7 and 8 apply to the middle, and the data in figures 9 and 10 apply to the high end of the band for which this coupling network was designed.

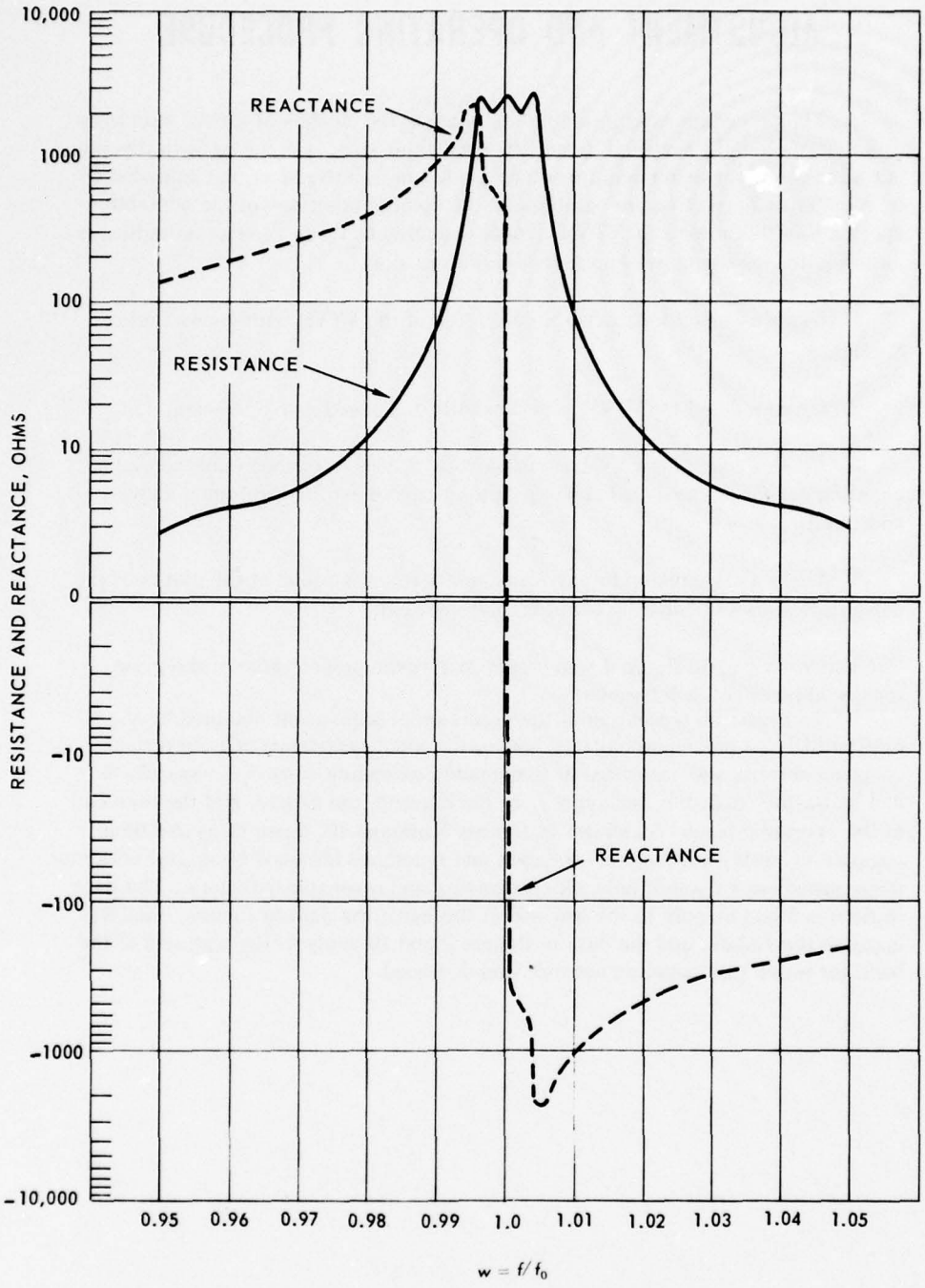

Figure 5. Computed input impedance of PAC-1A-1000 at 2.000 MHz.

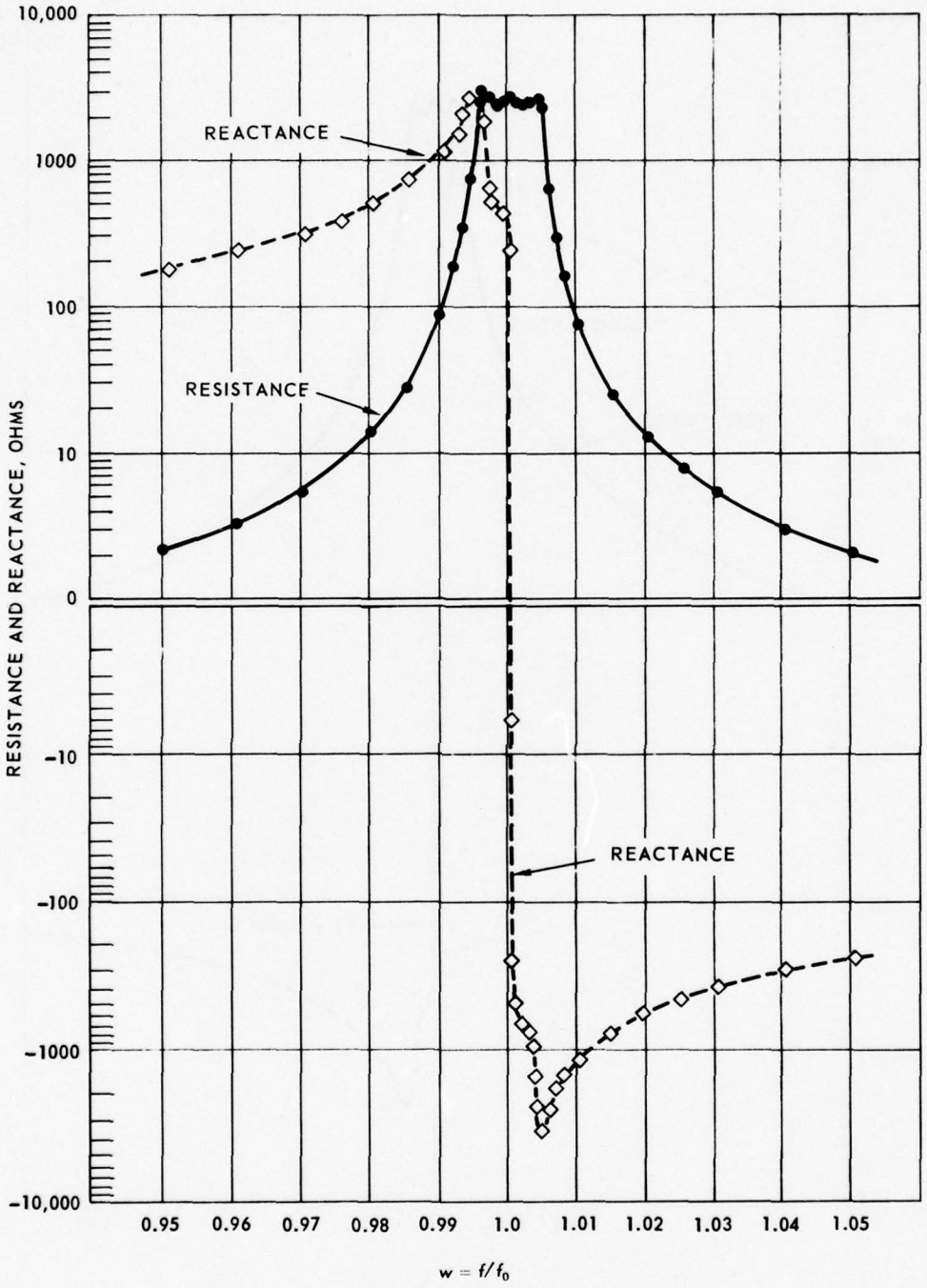

Figure 6. Measured input impedance of PAC-1A-1000 at 2.000 MHz.

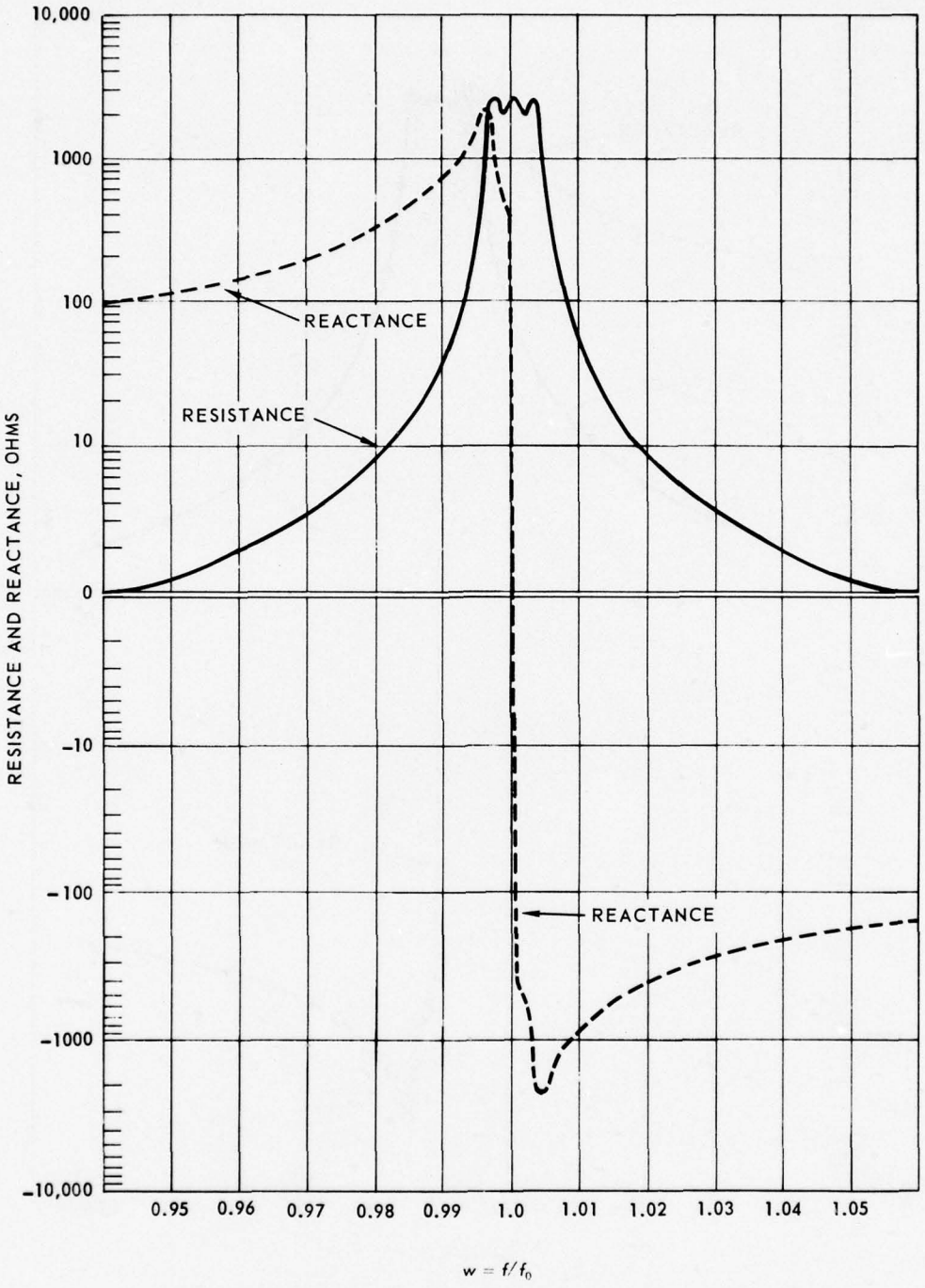

Figure 7. Computed input impedance of PAC-1A-1000 at 2.828 MHz.

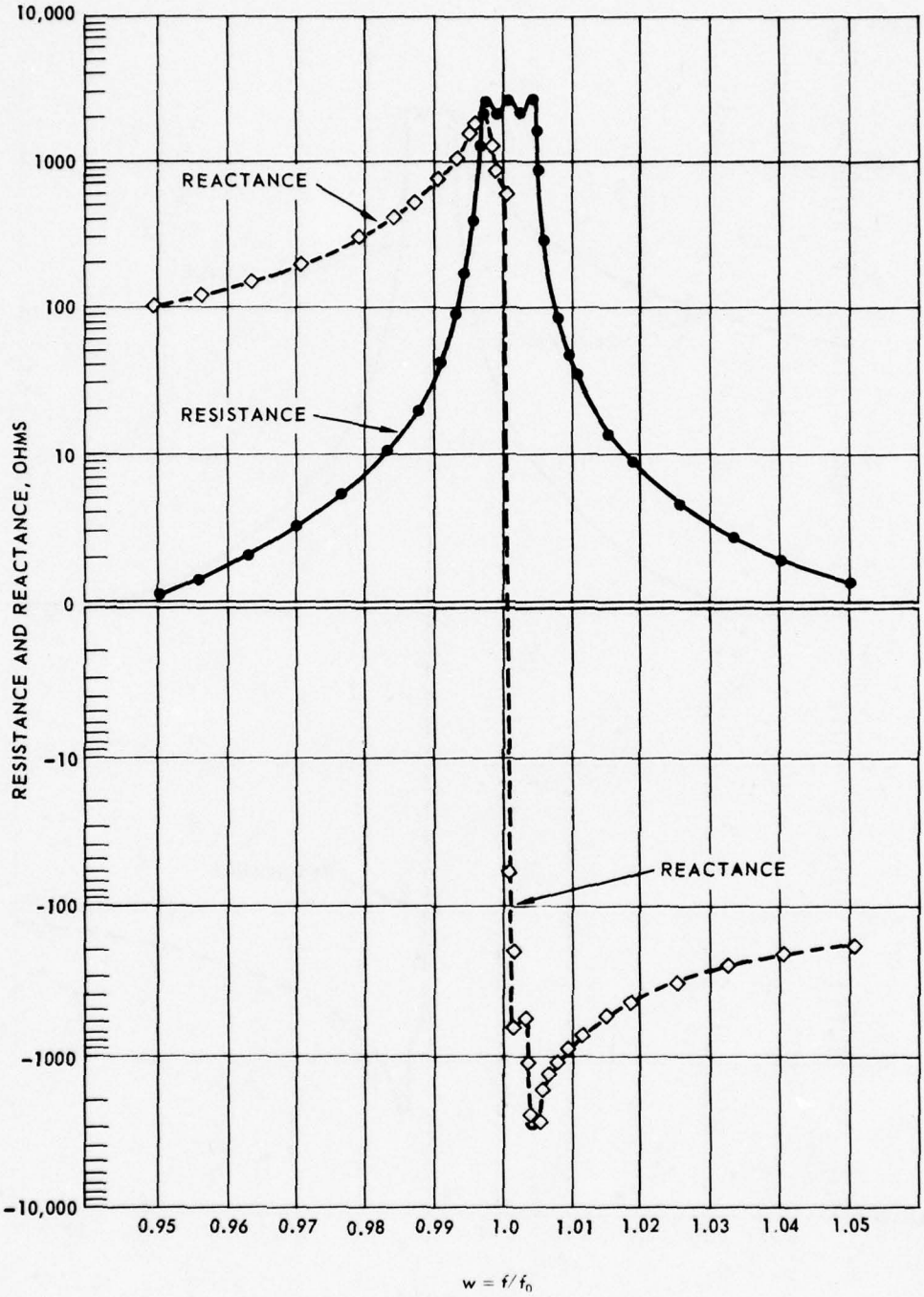

Figure 8. Measured input impedance of PAC-1A-1000 at 2.828 MHz.

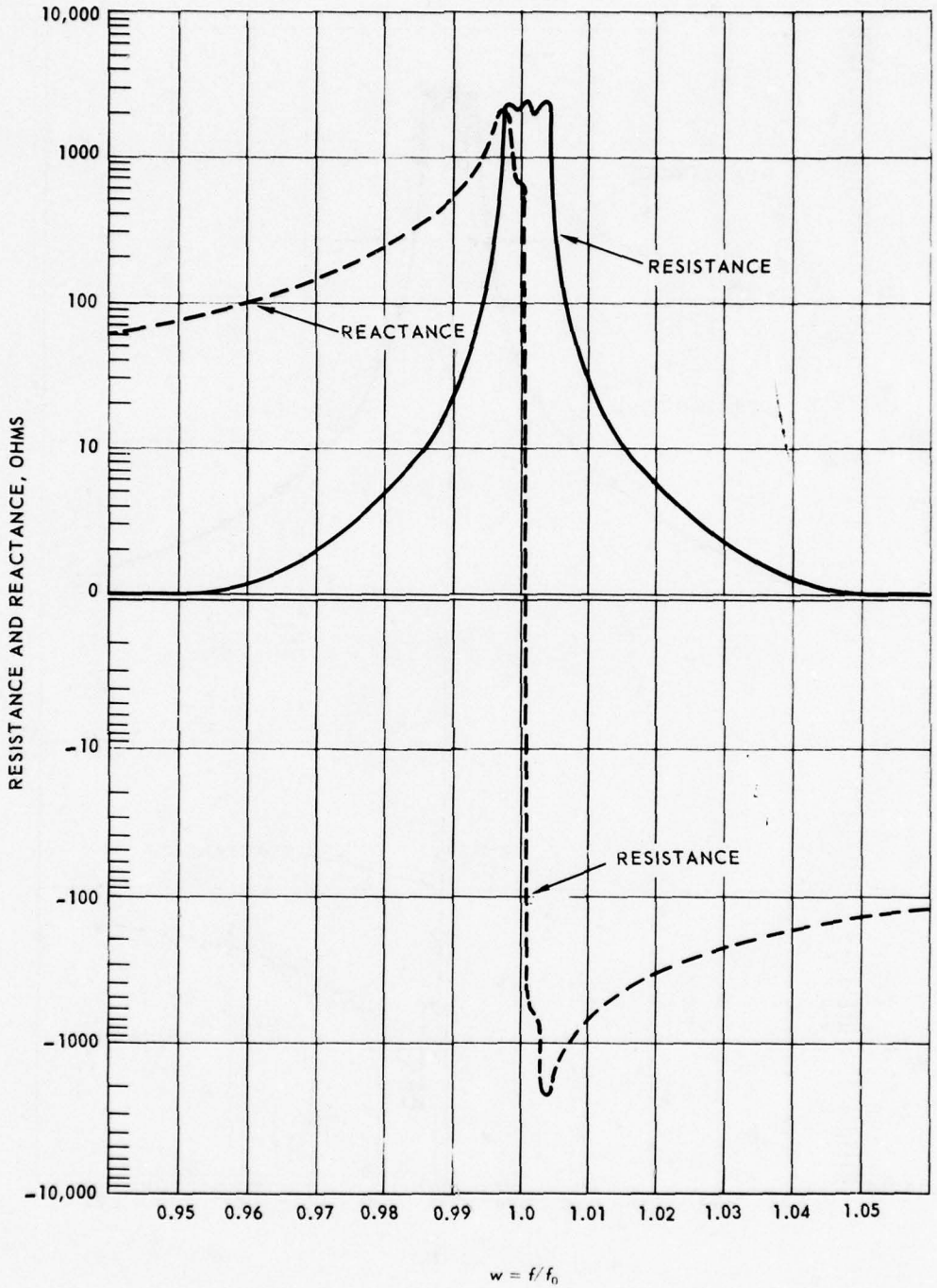

Figure 9. Computed input impedance of PAC-1A-1000 at 4.000 MHz.

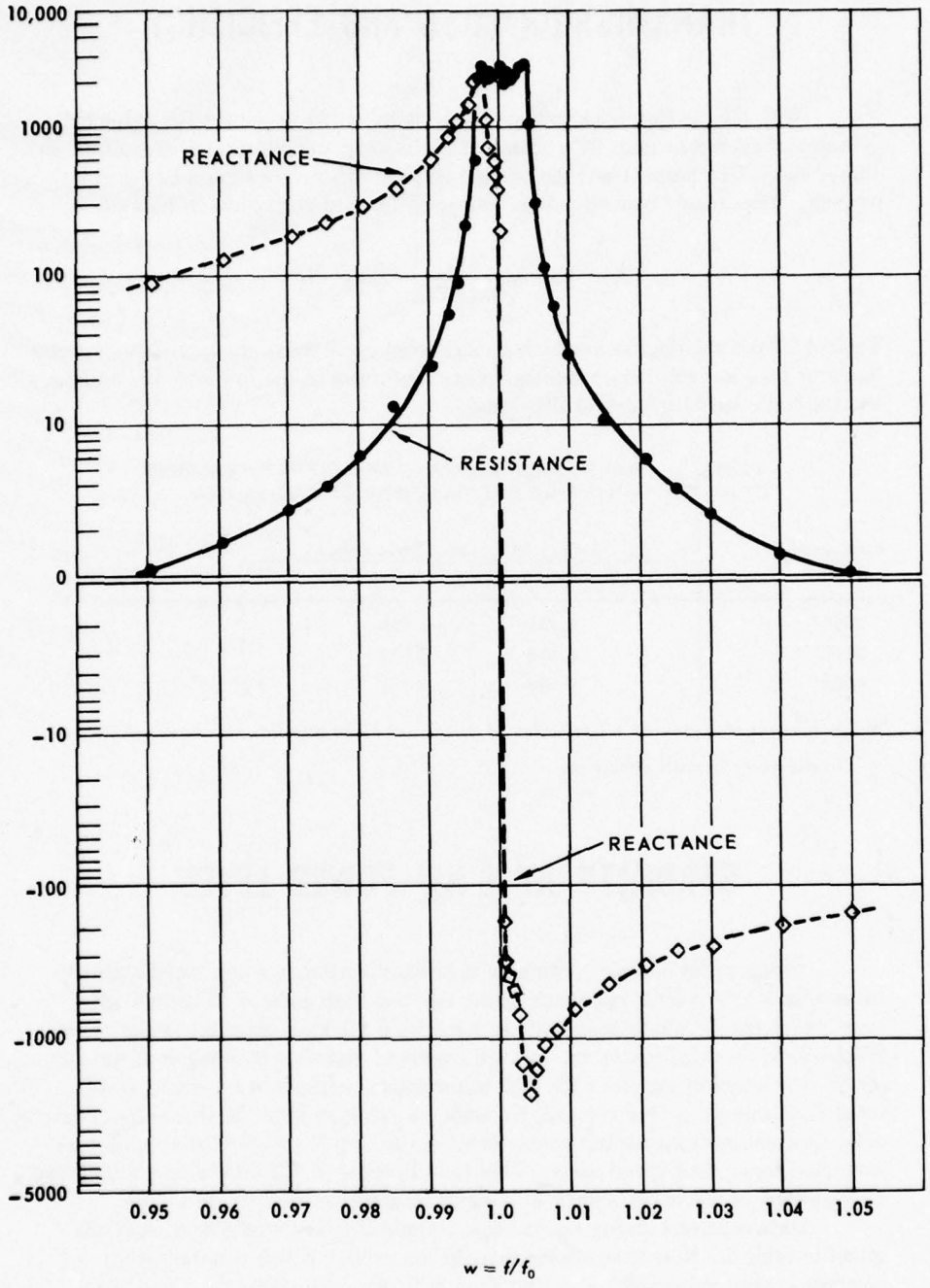

Figure 10. Measured input impedance of PAC-1A-1000 at 4.000 MHz.

TRANSMISSION LOSS AND EFFICIENCY

With the apertures and output coupling adjusted to reduce the unloaded Q-factor of each resonator by a factor of 7, the computed efficiency of each mesh should be 85.714 percent and the overall coupler efficiency should be 62.974 percent. This result corresponds with a total forward transmission loss of

$$L_f = 10 \log \frac{1}{0.62974} = 2.008 \text{ dB}$$

Table 1 shows the degree to which these design objectives are approached on the basis of loss and efficiency measurements performed at the low end, the middle, and the high end of the 2-to-4 MHz band.

TABLE 1. TRANSMISSION LOSS AND EFFICIENCY MEASURED AT THE CENTER OF THE PASSBAND OF PAC-1A-1000

Frequency (kHz)	Measured Coupler Efficiency*		Transmission
	$\eta_t' = \eta_1 \eta_2 \eta_3$	$\eta_t'' = P_L/P_{in}$	L_f' (dB)
2000	0.612	0.608	2.12
2828	0.618	0.618	2.09
4000	0.618	0.618	2.09

*η_t' = product of measured efficiencies of the three resonators

η_t'' = measured overall efficiency

STABILITY AT 5-KW POWER LEVEL

Using water and air cooling as described earlier, we performed stability tests with PAC-1A-5000 operating at the low and high ends of the 2-to-4 MHz band. With the 4CX5000 beam tetrode furnishing 5.1 kilowatts, the power in the 50-ohm load was 3.2 kilowatts. Having observed significant changes in the output of the IPA stage of the AN/FRT-39A transmitters, explained in part by rather large fluctuations in line voltage, we made an effort to hold the IPA output reasonably constant during stability measurements. A Bird Model 8781 rf coaxial load was used throughout these tests. This load is rated at 7.5 kilowatts when cooled by 4 gallons of water per minute at a water temperature of 30°C or less.

Data recorded during two continuous stability tests of 1 hour each are given in table 2. Note that efforts to keep the driving power constant were somewhat more successful at 4 MHz than at 2 MHz, reflecting the small time delay and experimental error inherent in reading incident and reflected power on a single reflectometer (requiring rotation of the sensing element). The data on input VSWR show that the input impedance of the PAC assembly was relatively constant throughout each test.

The greatest change observed during these tests was the increase of some 10 percent in PA plate current during the first 50 minutes of the 4 MHz run. Immediately after this test, the input capacitor (C_{1a} in figure 4) was readjusted to give minimum plate current. A reduction in capacity from 755.0 to 749.9 pF (a change of 0.68 percent) reduced the plate current from 1.60 to a (minimum) value of 1.50 amperes. A similar test showed that somewhat less detuning of the first mesh was experienced after an hour's operation at 2 MHz. Capacitor C_{1a} was reduced from 2050.0 to 2046.4 pF (a change of 0.18 percent) in reducing the plate current $\overline{I}_b$ from 1.39 to a minimum of 1.38 amperes. These small changes in C_{1a} may be due in part to temperature changes on the PA side of this large ceramic capacitor.

TABLE 2. OPERATING STABILITY OF POWER AMPLIFIER COUPLER AT 5-KW POWER LEVEL

Lapsed Time (minutes)	Excitation (watts)			Input	PA Currents		Output Power (watts)
	Incident Power	Reflected Power	Driving Power	VSWR	Plate (amp)	Screen (mA)	
(a) At low end of band (2.000 MHz)							
(start)	535	125	410	2.87	1.38	15.0	3250
5	525	120	405	2.83	1.39	15.0	3300
10	510	110	400	2.73	1.38	15.0	3200
15	510	110	400	2.73	1.38	15.0	3200
20	510	110	400	2.73	1.38	15.0	3200
25	520	115	405	2.77	1.39	15.0	3400
30	520	115	405	2.77	1.40	15.0	3400
35	515	115	400	2.79	1.39	15.0	3350
40	500	105	395	2.69	1.39	15.0	3300
45	515	115	400	2.79	1.40	15.0	3400
50	515	115	400	2.79	1.39	15.0	3400
55	510	110	400	2.73	1.38	15.0	3400
60	515	115	400	2.79	1.39	15.0	3400
(b) At high end of band (4.000 MHz)							
(start)	465	80	385	2.42	1.45	14.0	3200
5	465	80	385	2.42	1.45	15.0	3100
10	465	80	385	2.42	1.45	15.0	3100
15	460	80	380	2.43	1.46	15.0	3100
20	460	80	380	2.43	1.48	15.0	3100
25	460	80	380	2.43	1.50	15.0	3100
30	460	80	380	2.43	1.53	15.0	3100
35	460	80	380	2.43	1.55	15.0	3100
40	460	80	380	2.43	1.56	15.0	3100
45	460	80	380	2.43	1.58	14.5	3200
50	460	80	380	2.43	1.60	14.5	3200
55	460	80	380	2.43	1.60	14.5	3200
60	460	80	380	2.43	1.60	14.5	3200

In order to test the PAC at full-rated peak envelope power, a 20-minute test run was made with two sinusoidal (cw) excitation signals of 3998 and 4002 kHz, respectively. With approximately 10.2 kW (PEP) supplied at the plate

and 6.4 kW (PEP) at the dummy load, there was no indication of voltage breakdown or instability of operation. No corona discharge was visible, but a small audio tone could be heard inside the third (output) mesh. Investigation indicated that this tone originated from one of the Steatite insulators that supports the main inductor L_3 (perhaps from a small air gap between the ceramic and the metal cap secured to the coil). Since the coil is supported by other means (described in connection with figure 2), it seems likely that these Steatite insulators will prove to be unnecessary.

ATTENUATION CHARACTERISTICS

Multicoupler attenuation studies involve a number of special problems. Along with network components, proper consideration must be given to basic characteristics of the source and load; and in transmitting application, both the forward and reverse attenuation characteristics are of special interest. Some of these characteristics are extremely difficult – if not impossible – to measure accurately, necessitating a combination of analytical and empirical studies.

A brief description of the analytical approach and a few basic definitions will assist in understanding the results of these studies. The three-mesh PAC is first represented as an equivalent ladder. Assuming that the network is both linear and passive, we may readily obtain various branch currents and node-pair voltages with a digital computer assuming, say, unit voltage at either end. Of course, all circuit elements must be known from measurements or obtained from prescribed design conditions. Values of impedance are computed from corresponding voltages and currents at various nodes throughout the network. In computing reverse characteristics, we assume unit voltage at the plate-input terminals and the source of excitation is assumed to be at the nominal output terminals of the coupler.

Network analyses are greatly simplified when the source of energy can be accurately represented as a constant-voltage or constant-current generator. A high-power tube cannot be accurately represented in this manner, however, since its dynamic characteristics are both nonlinear and nonanalytic. To facilitate comparison with characteristics of conventional two-mesh coupling units that are often measured in a so-called 50-ohm system, computations have been extended to include effects of a constant-impedance generator that matches the PAC network at its various operating frequencies.

Several important forward and reverse characteristics of the three-mesh PAC assembly will be defined with reference to the generalized network in figure 11. Compared with the schematic in figure 4, terminals a and b are assumed to represent the PA plate and ground, while i and j denote terminals connected to a resistive load R_L. Effects of the parasitic suppression elements, rf choke, plate coupling capacitors, bypass capacitors, and distributed parameters were neglected in the computations. Apart from unavoidable experimental error, the comparative analytical and experimental results in this study show the general agreement that is realized under these simplifying assumptions.

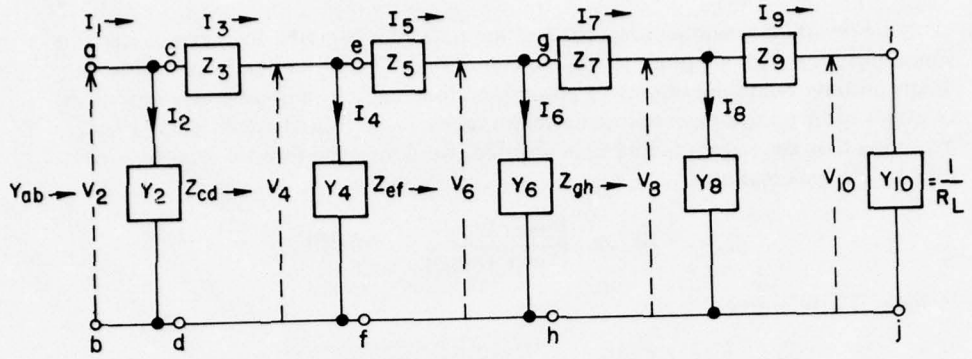

(A) ASSUMING UNIT VOLTAGE AT i-j (V_{10} = 1 VOLT)

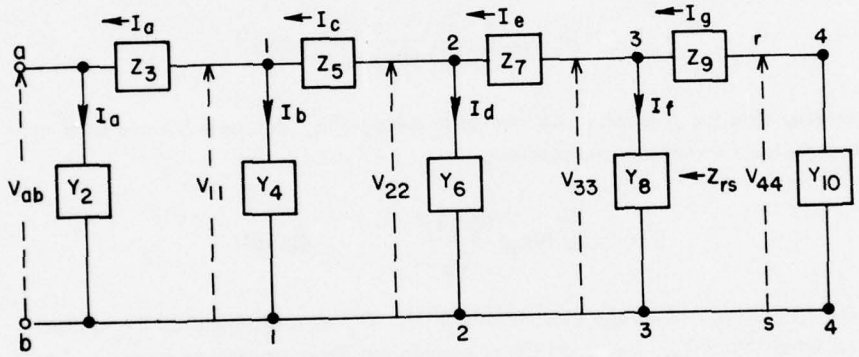

(A) ASSUMING UNIT VOLTAGE AT a-b (V_{ab} = 1 VOLT)

Figure 11. General network forms used in computing forward and reverse characteristics.

Forward attenuation properties of the networks describe their power transfer characteristics from the plate to the (antenna) load. The situation is complicated by uncertainty regarding effects of power tube loading.[3] In this program the problem is attacked by analyzing coupling networks under two different conditions: First, assuming that generator loading is negligible, we define the forward *transmission loss* by the expression,

$$L_f = 10 \log_{10} \frac{\text{Power Input}}{\text{Power Output}} \quad \text{(in dB)} \tag{1}$$

In figure 11, this gives

$$L_f = 10 \log_{10} \frac{P_{ab}}{P_L} \quad \text{(in dB)} \tag{2}$$

with Y_2 denoting the susceptance of the input capacitor C_{1a} in figure 4. Second, assuming that the network provides a purely conductive input equal to the generator's conductance G_g at the design or operating frequency f_o, we define *forward attenuation* as

$$L_a = 10 \log_{10} \frac{\text{Power Available}}{\text{Power Output}} \quad \text{(in dB)} \tag{3}$$

Assuming that the generator supplies unit voltage V_{10} across a 50-ohm load, we may compute forward attenuation from

$$L_a = 10 \log_{10} \frac{12.5\, I_1^2}{G_g} \quad \text{(in dB)} \tag{4}$$

where I_1 is supplied by the current source and G_g is combined with B_{1a} in the shunt admittance Y_2. Equation (2) is convenient for comparisons involving basic coupler-design criteria, being independent of the generator's impedance. Equation (4) is convenient in comparing PAC attenuation characteristics with coupler measurements using so-called standard (50-ohm) terminations. The selectivity actually achieved will probably fall somewhere between the characteristics given by equations (2) and (4).

Reverse attenuation characteristics of transmitting multicouplers are used to show the effectiveness of the networks in preventing cross-modulation in the system. With several signals present in the common load circuit, undesirable radiation products can originate from high-level modulation by energy fed from the load to the plates of various power amplifier tubes. Since these sources of energy are effectively in the antenna circuit, any reverse voltage at the plate obviously depends upon the output impedance of the power tube and this is another highly uncertain factor. In consequence, computations have been performed neglecting tube effects (i.e., assuming infinite output impedance) and also assuming a matched conductive termination G_g. Assuming a reverse voltage V_{ab}

of 1 volt in figure 11B and neglecting tube effects, the *reverse voltage attenuation* is given by

$$\alpha_r = 20 \log_{10} \frac{V_{44}}{V_{ab}} = 20 \log_{10} V_{44} \qquad \text{(log units)} \tag{5}$$

With $G_g + jB_{1a}$ forming Y_2, the *reverse power attenuation* is

$$L_r = 10 \log_{10} \frac{P_{rs}}{V_{ab}^2 G_g} = 10 \log_{10} \frac{P_{rs}}{G_g} \qquad \text{(in dB)} \tag{6}$$

with V_{ab} assumed constant at 1 volt.

Means for computing various impedance and power relationships are self-evident, if one knows the relative currents and voltages in figure 11 under unit-output conditions. Time limitations do not permit consideration of all these network characteristics in this study, so only those computed results that are most applicable to prescribed experimental tests will be included.

Figures 12 through 17 show measured and computed data giving the forward transmission loss characteristics of the three-mesh PAC at 2.000, 2.828, and 4.000 MHz. The values measured at these operating frequencies are identified by L_f' in table 1. Note that the data extend 5 percent above and below the nominal operating frequency, identified by frequency parameter $w = f/f_0 = 1$ in all cases. These curves show that the measured transmission loss 5 percent below f_0 is somewhat larger than the computed values, while the loss measured 5 percent above f_0 is smaller than the computed loss. Auxiliary tests indicate that this is due primarily to intercoupling between the first and third meshes of the PAC assembly. The cross-coupled energy is out of phase with the normally coupled energy below f_0, but these energy components are in phase above f_0. For best harmonic suppression it would be desirable if this situation were reversed and, therefore, it is desirable that cross-coupling effects be kept small.

Figure 18 gives computed data showing the difference between the forward loss characteristics of a three-mesh PAC with and without effects of a matched generator. The insert gives details in the vicinity of f_0. The influence of generator loading is seen to be appreciable at frequencies as little as 0.5 percent removed from the nominal operating frequency, the differences increasing with frequency separation. It is emphasized that the curve of L_a gives the relative power that would be delivered to a 50-ohm resistive load from an equivalent Thevenin's or Norton's generator, assuming that the coupling network matches the generator (i.e., accepts maximum power) at the design frequency f_0. The curve marked L_f, computed by equation (1) or (2) denotes the relative efficiency with which the network delivers power to the load. Figure 19 shows computed values of transmission loss for various terminal pairs *c-d, e-f,* and *g-h* in figure 11A. (Since C_{1a} and other network components in the PA plate circuit to the left of the dashed line in figure 4 are assumed lossless, the curves of L_f and L_{cd} in figures 18 and 19 are identical.)

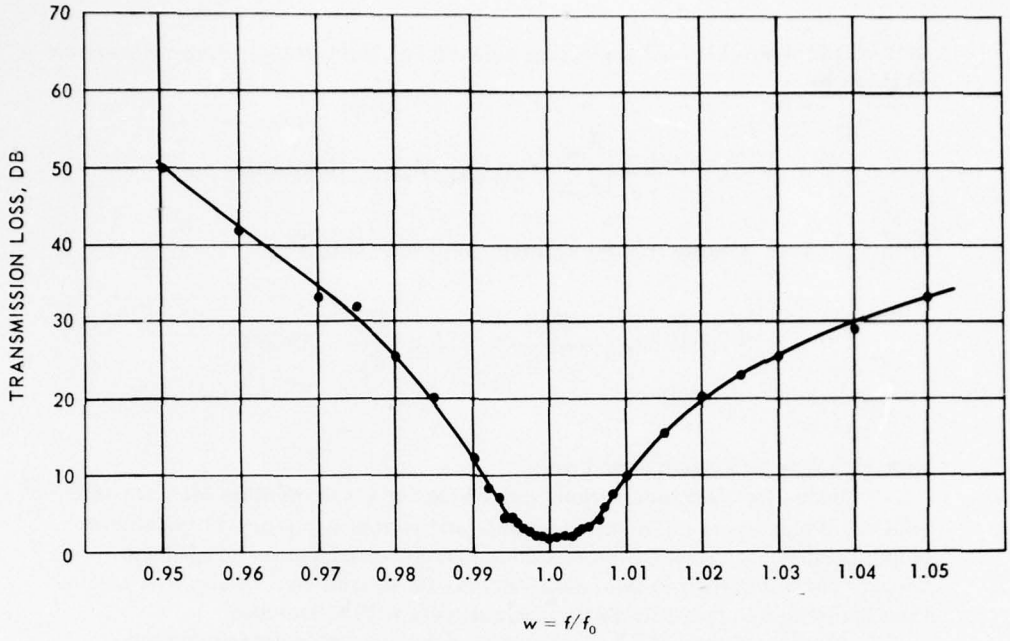

Figure 12. Transmission loss of PAC-1A-1000 measured at 2.000 MHz.

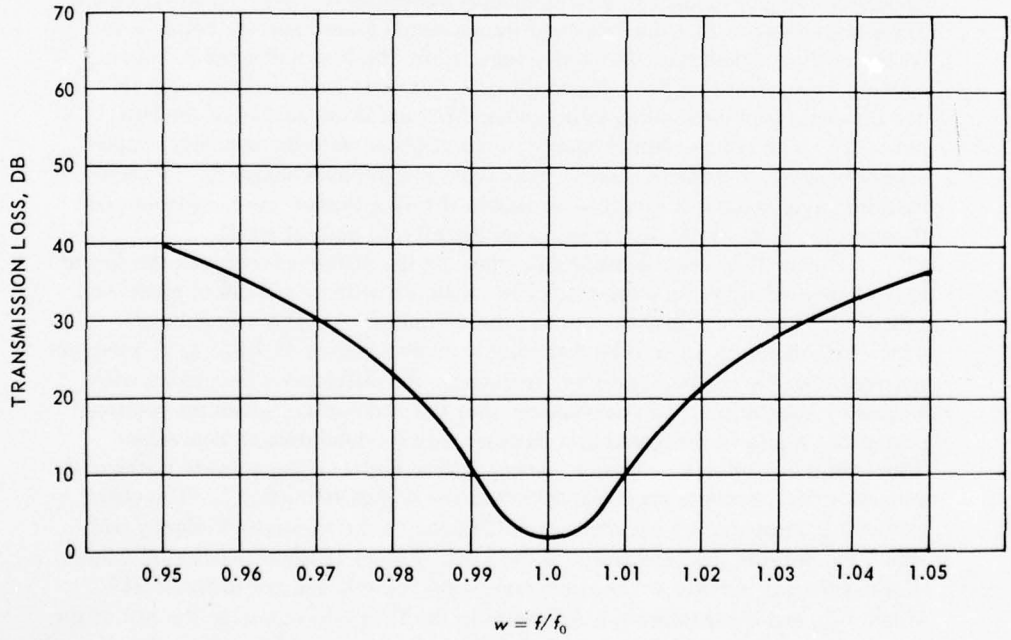

Figure 13. Transmission loss of PAC-1A-1000 computed at 2.000 MHz.

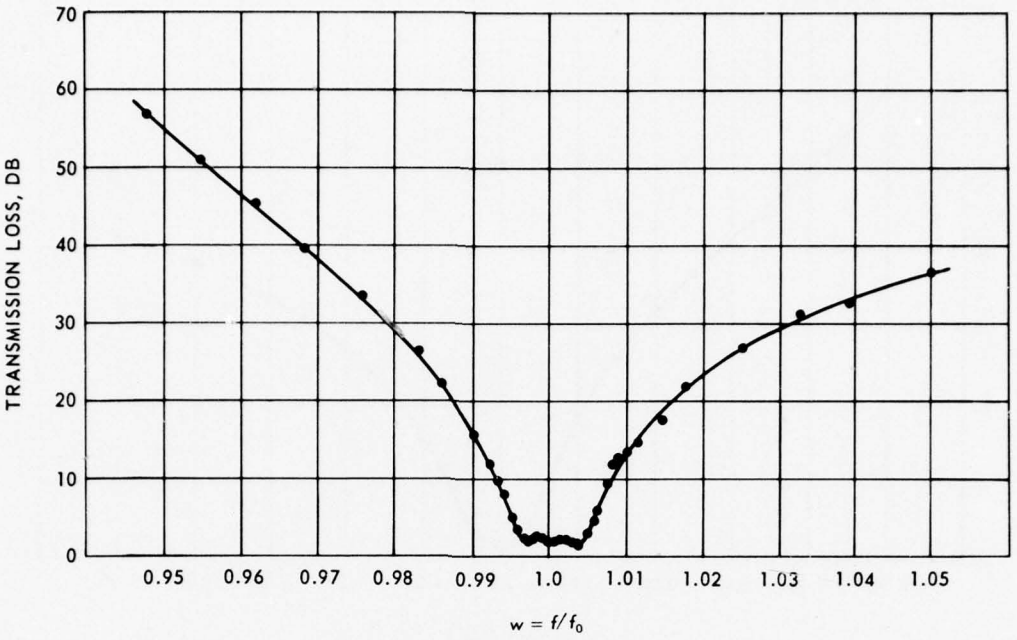

Figure 14. Transmission loss of PAC-1A-1000 measured at 2.828 MHz.

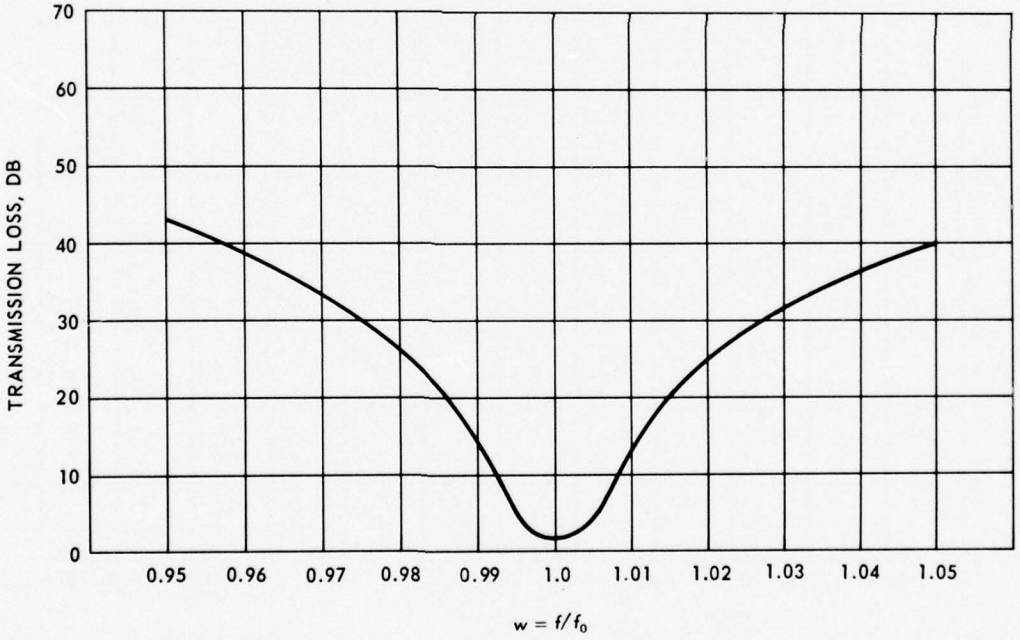

Figure 15. Transmission loss of PAC-1A-1000 computed at 2.828 MHz.

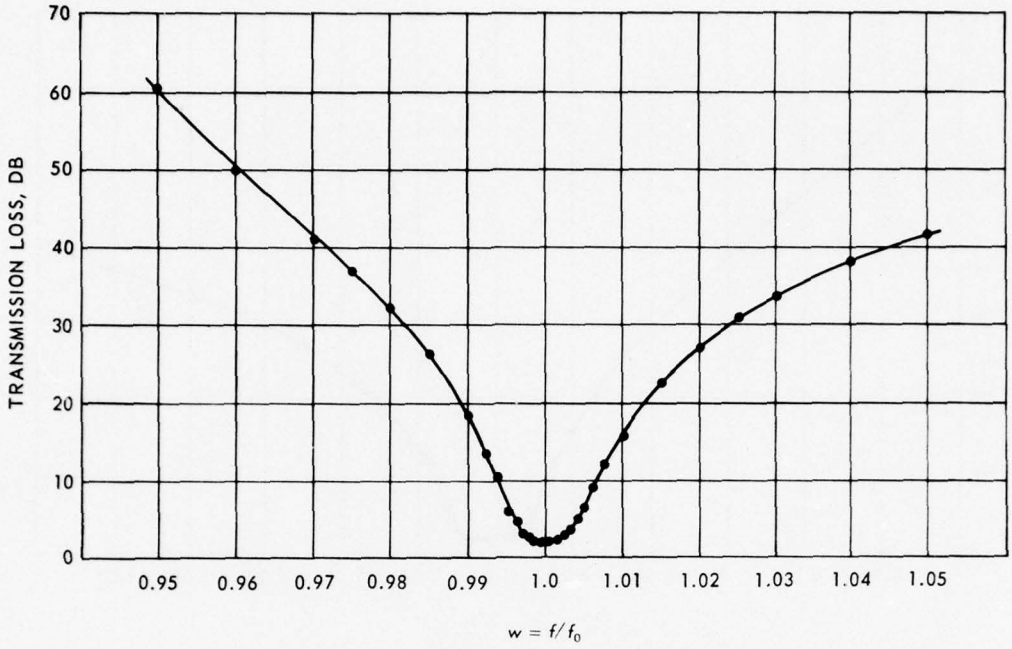

Figure 16. Transmission loss of PAC-1A-1000 measured at 4.000 MHz.

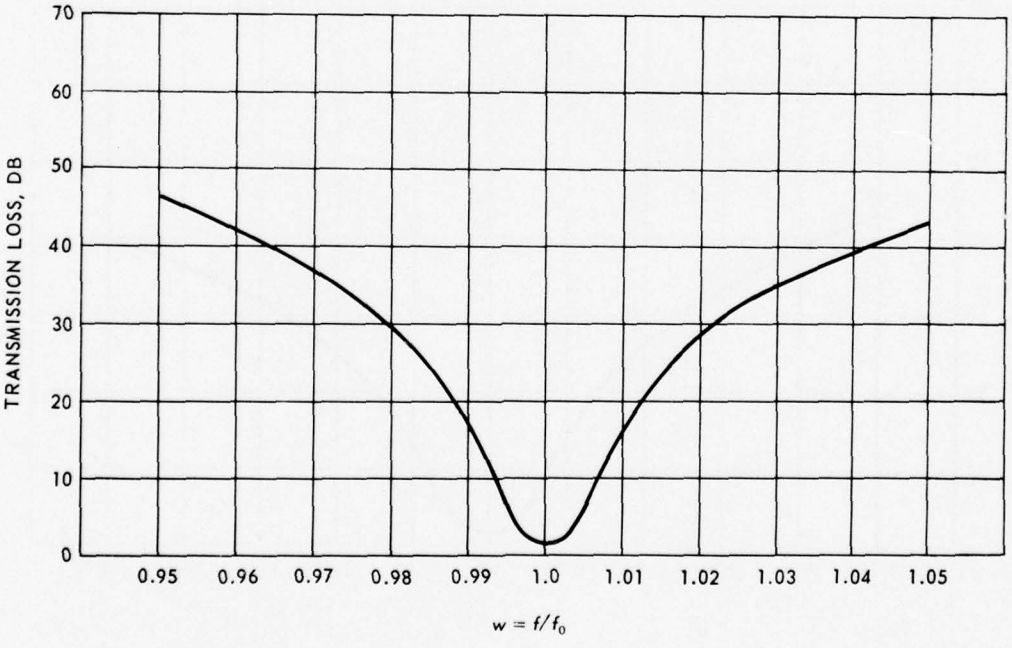

Figure 17. Transmission loss of PAC-1A-1000 computed at 4.000 MHz.

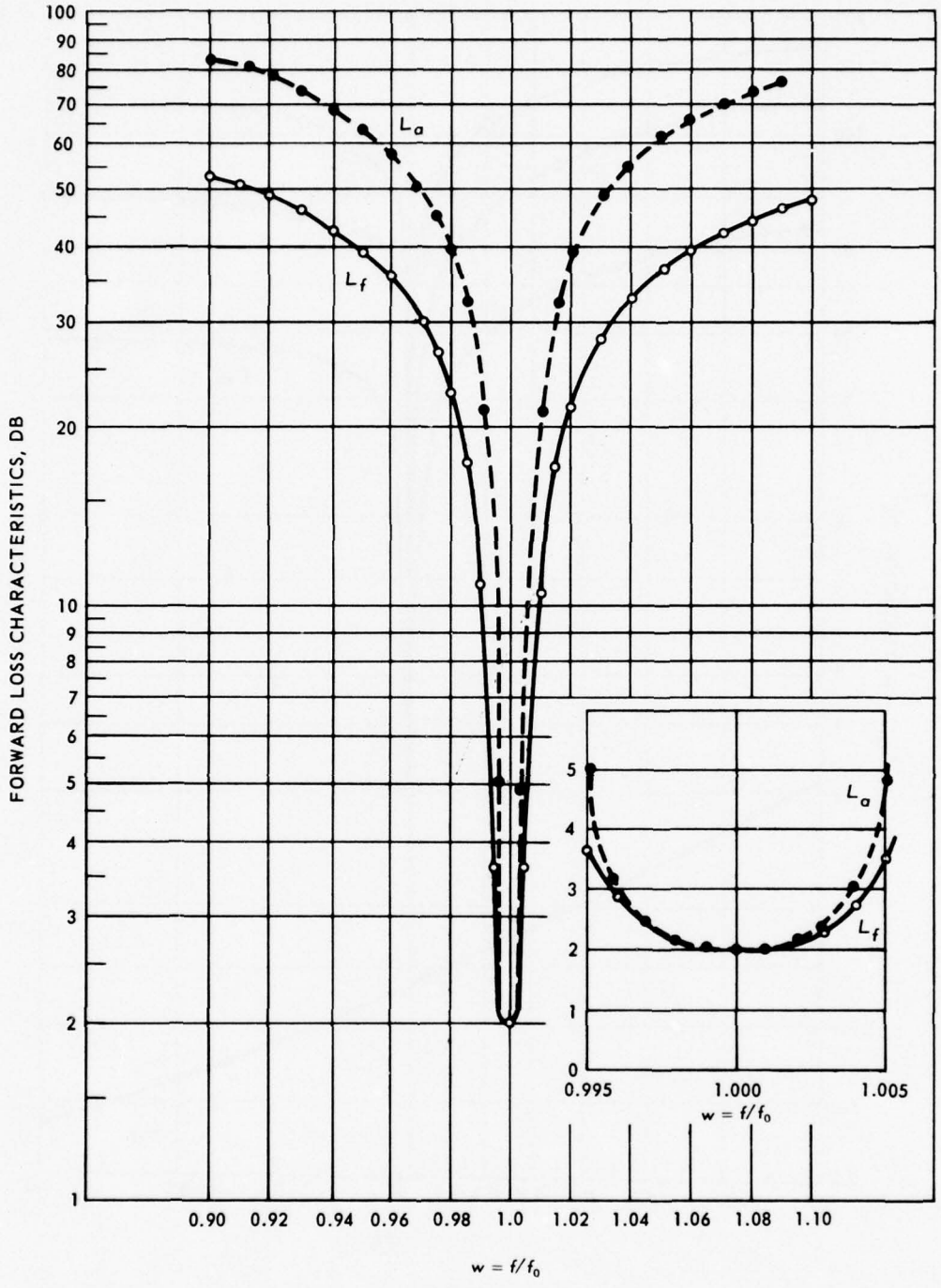

Figure 18. Curve (L_a) showing the effects of a matched generator on the transmission loss (L_f) computed using equation (2).

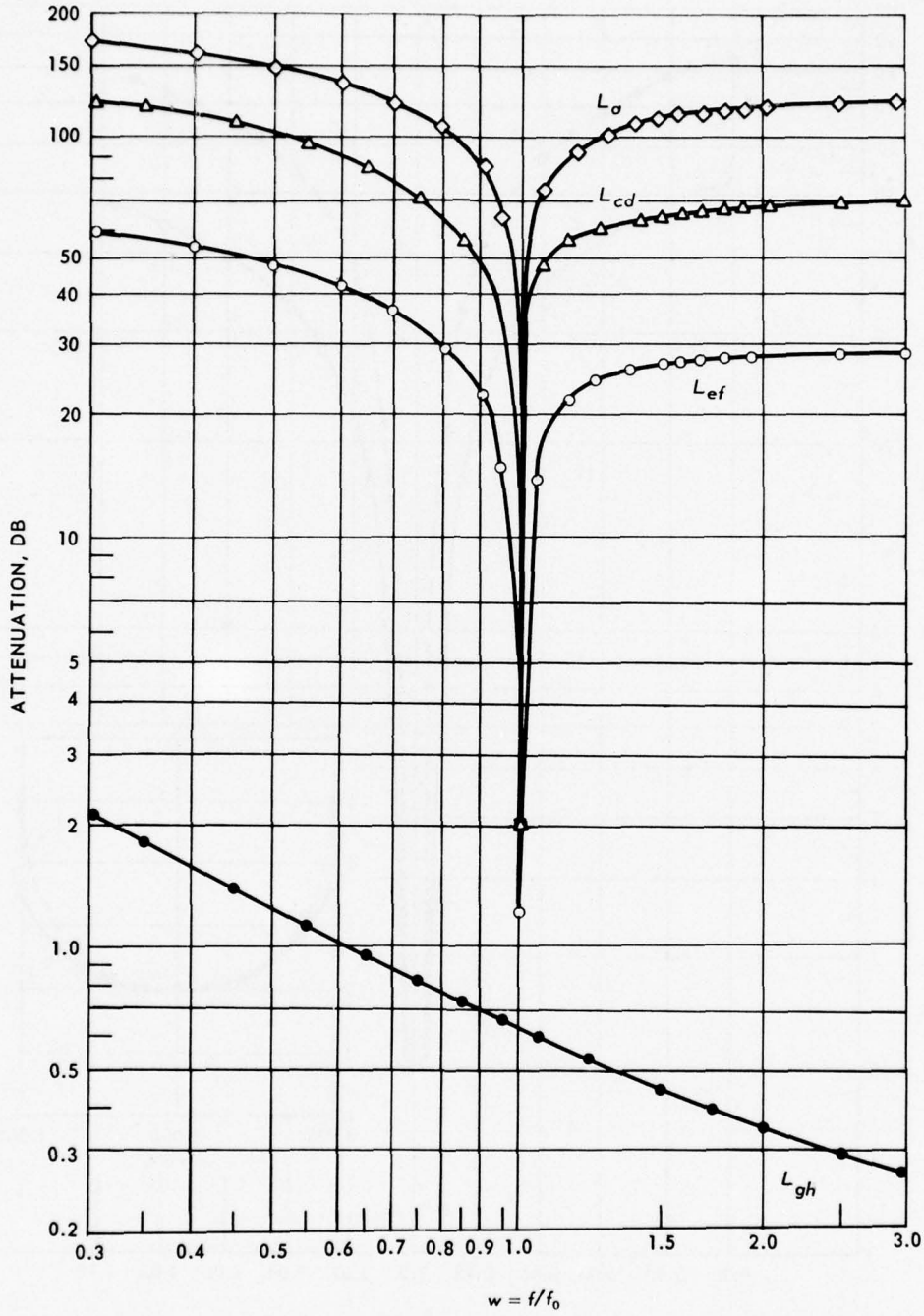

Figure 19. Computed transmission loss characteristics at points indicated by letters in figure 11A. Additionally, the curve of L_a is included to indicate effects of generator loading.

The relative performance characteristics of a PAC assembly composed of either two or three resonators are of special interest. As explained earlier, it is relatively simple to delete or add a resonator unit of the type shown in figure 3 in experimental tests of PAC assemblies illustrated in figures 1 and 2. Consequently, transmission loss measurements were performed at 2 and at 4 MHz using both two-mesh and three-mesh PAC assemblies. The results are summarized in table 3.

TABLE 3. TRANSMISSION LOSS OF TWO-MESH AND THREE-MESH POWER AMPLIFIER COUPLERS MEASURED AS A FUNCTION OF PERCENTAGE SEPARATION FROM THE NOMINAL OPERATING FREQUENCY (EXPRESSED IN dB)

Separation from f_0 →	−5.0%	−2.5%	0%	+2.5%	+5.0%
a. Using nominal operating frequency of 2.000 MHz					
Two-Mesh PAC	15.4	9.98	1.34	10.2	15.8
Three-Mesh PAC	50.0	30.5	2.0	23.0	33.5
b. Using nominal operating frequency of 4.000 MHz					
Two-Mesh PAC	16.6	11.6	1.42	12.6	19.3
Three-Mesh PAC	60.5	37.5	2.10	30.5	41.5

The attenuation properties of the PAC assemblies have been investigated briefly at frequencies extending throughout the hf band. Because of practical difficulties in directly exciting these highly selective circuits at the plate terminals when the frequencies are some 5 percent or more removed from the operating point, these general stop-band properties have been analyzed in an indirect manner. The approach is indicated in figure 20. The AN/SRT-16 radio transmitter was connected to the output link through a 50-ohm dummy load. The power supplied at each frequency was computed from measured values of output impedance Z_{rs} ′ and voltage V_i identified in the figure. With a "noninductive" resistor R_g connected from plate to ground, the reverse power was computed using readings from millivoltmeter V_0. In view of the large uncertainty in V_0 (in the presence of some 6 millivolts of noise) and other unavoidable errors, the measured data in table 4 are at best approximations intended primarily to indicate the absence of significant nulls in the attenuation characteristic at the higher frequencies in the 2-to-30 MHz band. This conclusion is supported, also, by similar empirical measurements performed with the PAC assembly tuned and loaded at 4 MHz. Supplementary tests showed that secondary attenuation nulls do exist above 30 MHz, depending somewhat upon PAC adjustments. When tuned to 2 MHz, the attenuation of the PAC dropped to about 35 dB at 32.9 MHz; and when tuned to the 4 MHz, an attenuation null of some 42 dB was indicated at 33.2 MHz. The foregoing are values of attenuation relative to the response at f_0. These nulls appear to be related to the self-resonant frequencies of the main resonator inductors which occur around 33 MHz in this instance, as indicated by a grid-dip meter.

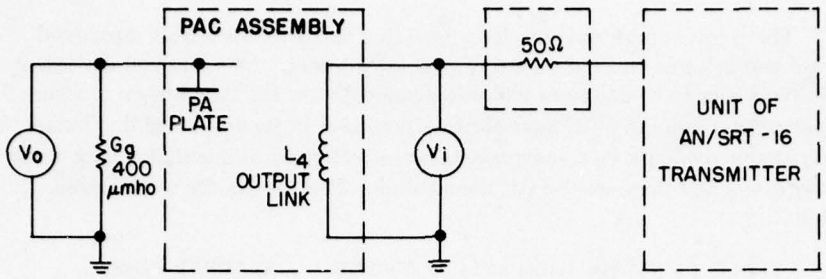

Figure 20. Instrumentation used in exploring the (reverse) attenuation characteristics of the PAC from 2 to 30 MHz.

TABLE 4. SOME MEASURED AND COMPUTED TRANSMISSION LOSS CHARACTERISTICS OF THE PAC AT FREQUENCIES CONSIDERABLY REMOVED FROM THE OPERATING FREQUENCY (2 MHz)

Test Frequency (MHz)	$w = \frac{f}{f_0}$	G_{rs}' (measured in μ mho)	Reverse Loss L_r (dB)		Forward Loss (computed in dB)
			Measured	Computed	
2.100	1.050	12,300	34.7	37.92	36.66
2.500	1.250	1,740	70.1	63.70	59.42
3.000	1.500	1,060	*	73.62	66.19
5.000	2.500	410	*	87.45	71.37
8.450	4.225	148	*		
10.000	5.000	101	72.1		
15.000	7.500	34.6	70.4		
20.000	10.000	28.2	65.6		
25.000	12.500	19.5	62.8		
27.000	13.500	19.5	66.1		

Note 1 - The (*) signifies that the desired signal was masked by noise.
Note 2 - No computations were performed with $w > 3$.

The computed values of forward and reverse transmission loss in the two right-hand columns of table 4 serve to emphasize that these loss characteristics are not identical. Thus, even assuming optimum source and load terminations, the selectivity characteristics of a PAC assembly depend somewhat upon the direction of power flow. The explanation is simple: matched conditions do not normally exist at both input and output terminals. With extremely different impedance levels at the source and load, a perfect "match" at both input and output requires a particular relationship between the intrinsic loss components of the circuits. For example, assuming two inductively coupled circuits with effective

(series) generator and load resistances R_g' and R_L', respectively, the loss components of the circuits must satisfy the relationship,

$$\frac{R_g'}{R_L'} = \frac{r_1}{r_2} \tag{7}$$

if both circuits are resonant (i.e., $X_{11} = X_{22} = 0$).

The measured and computed values shown in figure 21 and in table 5 illustrate several impedance relationships applicable to one of the PAC assemblies under test. On the basis of the measured values of unloaded Q's, the circuit was designed to present a purely resistive load of 2500 ohms to the plates of two 3-400Z power triodes employed in early studies. The internal coupling coefficients were chosen to reduce these values of Q_u by a factor of 7, as noted earlier. The digital computations were carried to ten significant figures, but certain values in table 5 have been rounded off at six figures or less because of space limitations. With a 50-ohm resistive load, the desired 2500-ohm input is seen to be realized quite closely. On the other hand, with R_g of 2500 ohms

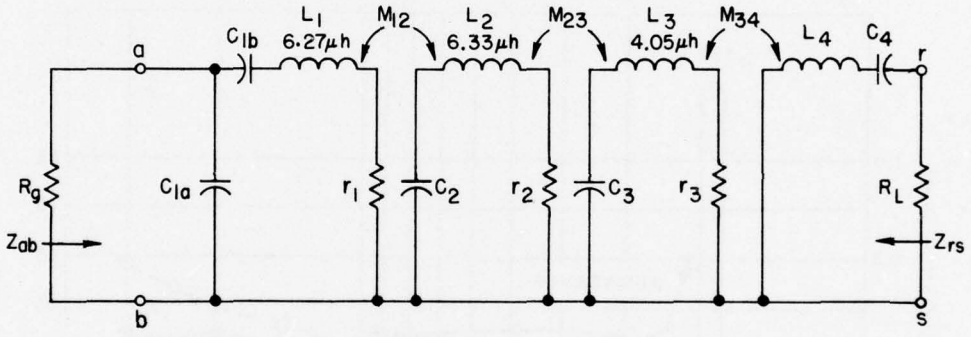

Figure 21. Simplified diagram of a "three-mesh" PAC designed for testing from 2 to 4 MHz (other measured and computed parameters are given in table 5).

TABLE 5. MEASURED VALUES OF UNLOADED Q-FACTORS AND COMPUTED VALUES OF INPUT AND OUTPUT IMPEDANCE OF THE NETWORK IN FIGURE 21 DESIGNED AND ADJUSTED FOR 2500-OHM PLATE-LOAD RESISTANCE AT EACH FREQUENCY

Frequency (MHz)	Measured Q-Factors			Z_{ab} (ohms) with R_L = 50	Z_{rs} (ohms) with R_g = 2500	Z_{rs}' (ohms) with $R_g = \infty$
	Q_{u1}	Q_{u2}	Q_{u3}			
2.000	994	980	847	2500.00 − j0.0091	38.87 − j 0.00017	151.31 + j8.06
2.828	1232	1211	1008	2500.00 + j0.0002	38.86 + j0.00000	151.24 + j8.73
4.000	1463	1449	1232	2500.00 + j0.0000	38.86 + j0.00000	151.17 + j9.27

connected across the input terminals a-b, table 5 shows computed values of Z_{rs} (the impedance looking left at terminals r-s in figure 21) to be about $38.86 + j0$ in each instance. Clearly, this would not match a 50-ohm generator in reverse power measurements and explains the fact that the reverse transmission loss is 1.9396 dB with a 2500-ohm termination whereas the forward transmission loss is 2.0084 dB with a 50-ohm termination.

Further evidence of the absence of undesirable moding of the PAC assembly is furnished by the stop-band impedance characteristics in figures 22 and 23. These data were measured at the plate terminals after the network had been adjusted for proper operation at 2 and 4 MHz with a 50-ohm load. Note that the resistive component remains quite small throughout the 2-to-30 MHz band except, of course, near the operating frequencies.

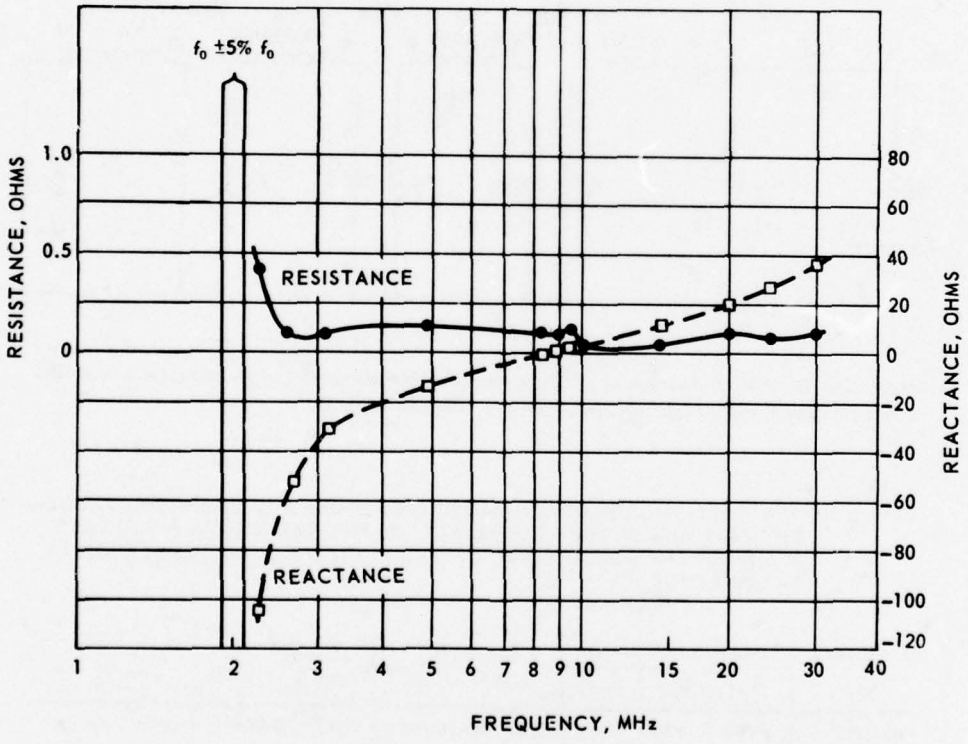

Figure 22. Measured components of stop-band impedance of PAC-1A 1000 tuned to 2.000 MHz.

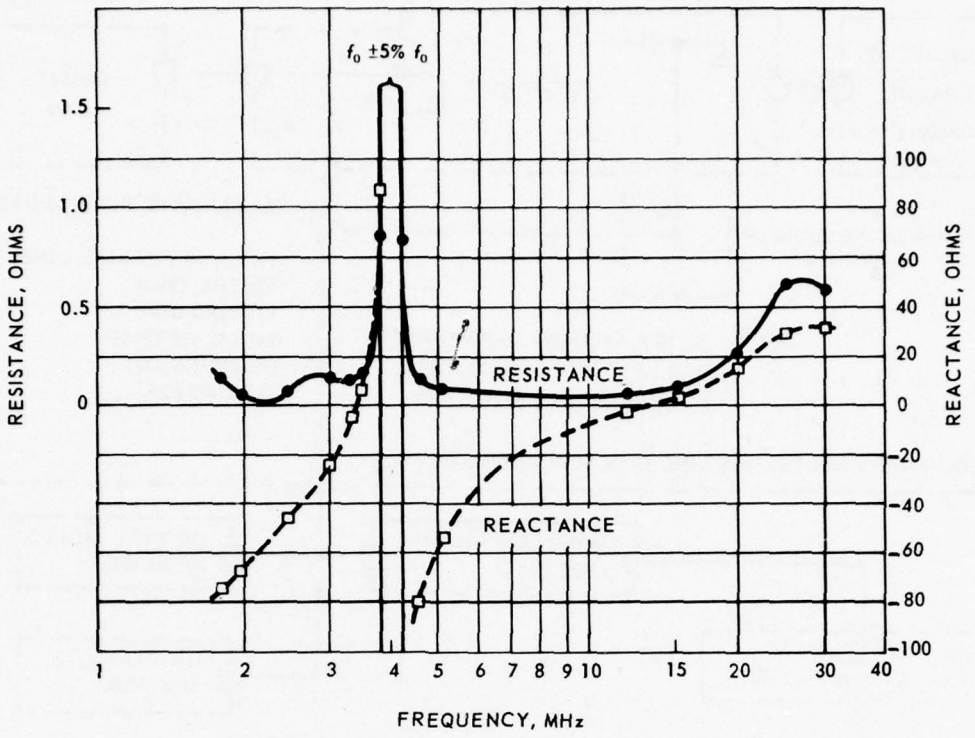

Figure 23. Measured components of stop-band impedance of PAC-1A-1000 tuned to 4.000 MHz.

ATTENUATION OF HARMONICS

Much time and effort were spent attempting to develop a technique that would give accurate and consistent harmonic measurements. The instrumentation used at the outset is indicated in figure 24. Various voltage divider schemes were tried. A 1000:1 capacitive divider was used to indicate the levels of various low-order harmonics at the plates of the two 3-400Z power triodes used in PAC-1A-1000. After trying several voltage-divider arrangements at the main 50-ohm dummy load, the use of a 70-watt 1210-ohm metal deposited resistor R_1 in series with the 50-ohm measuring line was finally adopted. To insure proper termination of this line in the screened room, the two-section bandpass filter was adjusted to present an input impedance of approximately 50 ohms (resistive) at each measurement frequency using the rf bridge. The use of terminating "pads" was held to a practical minimum in order to achieve maximum dynamic range from the measuring system.

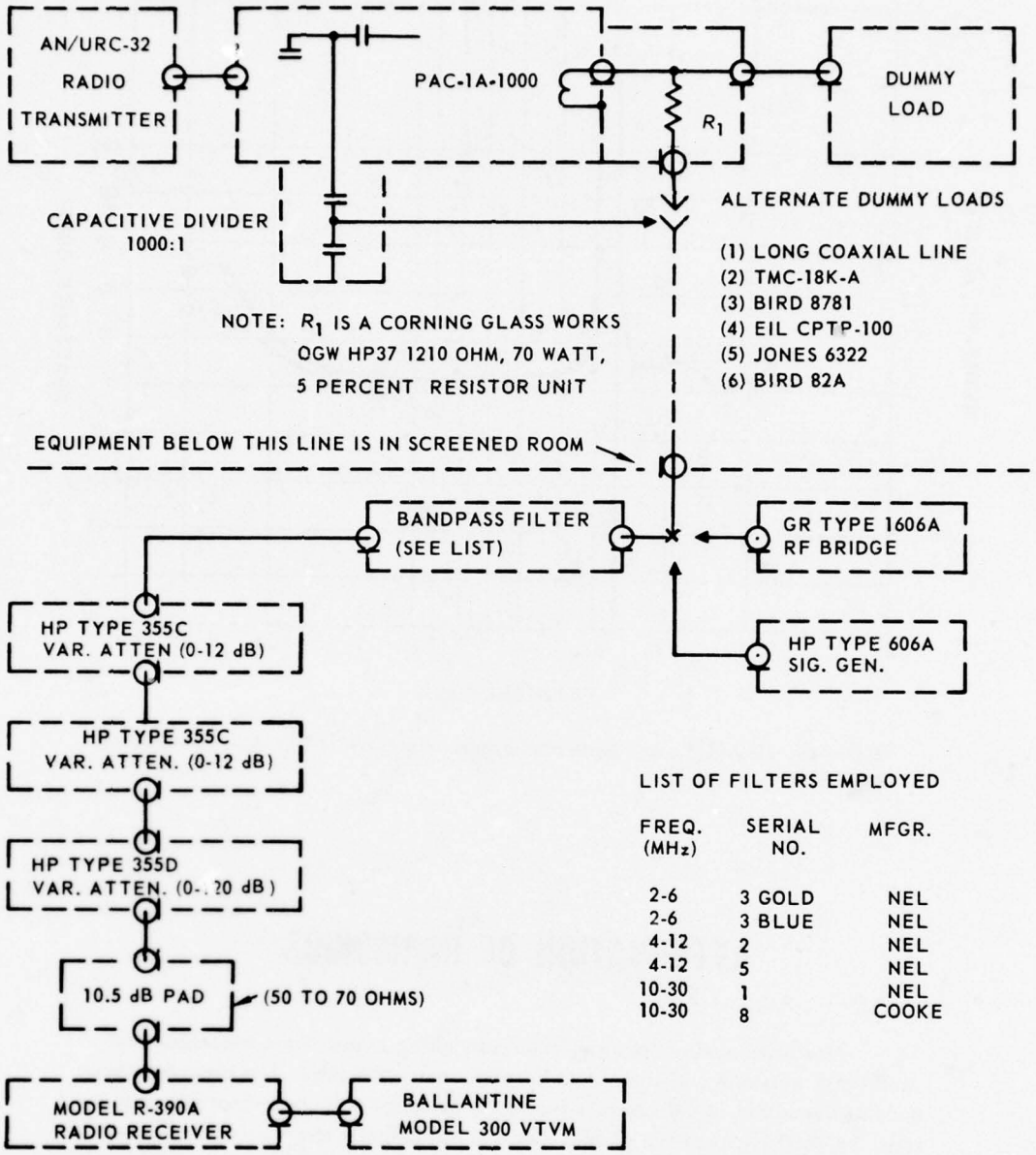

Figure 24. Block diagram of experimental setup used in measuring level of major harmonic signals from a 1-kilowatt PAC assembly.

The sensitivity of the system was controlled at each frequency of measurement by the following procedure:

1. The noise reference level was established with no signal input by setting the receiver's gain controls to give a reading of 0.2 volt (6 dB) on the VTVM. During these adjustments the signal generator was connected and the variable attenuators were set to zero.

2. A 10 dB signal-plus-noise-to-noise ratio was established by adjusting the signal generator's output to give a reading of 0.63 volt (16 dB) on the VTVM. The antenna trimmer on the receiver was adjusted for peak VTVM reading at each frequency.

3. The filter's coupling and tuning controls were adjusted for an input of approximately $50 + j0$ using the rf bridge. With the filters adjusted in this manner, separate tests showed their midband insertion loss to range from 3 to 4 dB at the frequencies employed in these tests. Thus, with an additional 10.5 dB of fixed loss introduced by the impedance-matching pad at the receiver's input, there was a total of roughly 14 dB of residual loss in the system.

By means of the instrumentation in figure 24, the levels of the second, third, and fourth harmonics were measured relative to the 500-watt power output supplied by the PAC assembly at 2 and 4 MHz. A direct substitution technique was employed. With a measured power of 500 watts into the 50-ohm dummy load at the fundamental frequency, the variable attenuators were adjusted for 10 dB (S+N)/N ratio. This required the addition of 134 dB of attenuation in each case, thereby establishing the dynamic measuring range of the system. The data in table 6 show the amount by which this variable attenuation had to be reduced to maintain the same reference level on the Ballantine VTVM at the various harmonic frequencies.

TABLE 6. MEASUREMENT OF RELATIVE HARMONIC LEVELS OF THREE-MESH AND TWO-MESH 500-WATT PAC, USING INSTRUMENTATION IN FIGURE 24

Operating Frequency f_0 (MHz)	DB Level of Harmonic Signals at Load Relative to Power at Fundamental		
	At $2f_0$	At $3f_0$	At $4f_0$
	(a) Using three-mesh PAC-1A-1000		
2.0	−134*	−133	−134*
4.0	−134*	−134*	−134*
	(b) Using two-mesh PAC-1A-1000		
2.0	−108	−113	−134*
4.0	−126	−127	−132

Note: The (*) denotes the fact that the harmonic level was equal or below the measuring capability of the system at the 500-watt level.

For the three-mesh PAC, table 6 shows that all harmonics tested were about 134 dB or more below the fundamental signal at both 2 and 4 MHz. The need for greater dynamic measuring range is self-evident; but, since the problem objective called for measurements at a much higher power level, no further attempt was made to increase the measuring range of this setup. Tests were extended, however, to indicate the harmonic attenuation of the two-mesh PAC configuration, with the results shown in the (b) part of table 6.

It is interesting to compare the (doubtful) second harmonic levels in table 6 with the values predicted by computer analysis, for the particular PAC network under consideration. As shown in the right-hand column in table 7, a total forward attenuation near 135 dB is computed at 4 MHz when operating at 2 MHz and the expected second-harmonic attenuation is some 10 dB larger at 8 MHz when operating at 4 MHz. Effects of cross-coupling, as explained earlier, would be expected to reduce these values somewhat.

TABLE 7. LEVEL OF SECOND HARMONIC ENERGY MEASURED AT PLATES OF TWO 3-400Z POWER TRIODES WITH RELATED COMPUTATIONS OF LOSS CHARACTERISTICS OF THREE-MESH PAC

Operating Frequency f_0 (MHz)	Harmonic Measured at Plates L_{ab} (dB)	PAC Data Computed at Second Harmonic Frequency			
		Plate-Load Impedance $R_{ab} + jX_{ab}$ (ohms)	Level at Plates L_{ab}' (dB)	Trans. Loss of PAC L_{cd} (dB)	Total Forward Attenuation L_f (dB)
2.0	−47.4	0.0042309−*j* 22.76007	−64.81	−70.25	−135.06
4.0	−63.9	0.0018531−*j* 24.69986	−68.39	−77.30	−145.69

Note: With the two tubes supplying rated power output of 1330 watts, the ratio of the second harmonic to the fundamental component of plate current is assumed to be 0.442 (as obtained from 13-point Chaffee analysis).

The measured and computed data in table 7 were obtained using a three-mesh PAC assembly with a pair of 3-400A power triode tubes operating in a grounded-grid circuit. Normal operation with 3000 volts on the plate was assumed, the plate power output being 1330 watts. Using the Chaffee 13-point harmonic analysis[4] with published constant-current characteristics of these tubes, the ratio of second-harmonic to fundamental component of plate current was found to be:

$$\frac{(I_p)_2}{(I_p)_1} = 0.442 \tag{8}$$

with the two tubes supplying 1330 watts to a resistive load of 2500 ohms. The rms value of $(I_p)_1$ is readily computed from the power output and load resistance. The value of $(I_p)_2$ is then obtained from (8), and the power supplied to the PAC network is computed using the value of input resistance R_{ab} given in the third column of table 7. When compared with 1330 watts, this gives the level of second harmonic energy L_{ab}' at the plates. Computed values L_{ab}' in column four

of table 7 are to be compared with measured values L_{ab} in column two, obtained by using the 1000:1 capacitive divider in conjunction with the screened-room instrumentation in figure 24. The agreement is much better at 4 MHz than at 2 MHz. If the harmonic energy at the plates and the forward transmission loss of the coupler can be correctly established, the sum of these quantities obviously gives an accurate determination of the total harmonic attenuation of the complete assembly.

Several harmonic measurements were made with a three-mesh PAC operating at higher power levels with a 4CX5000A beam tetrode in a "grounded-grid" circuit. Polarizing potentials of 1250 volts on the screen and -280 volts on the grid were obtained from an AN/FRT-39A transmitter. Initial tests were performed using the instrumentation in figure 24. For the direct substitution technique described earlier, table 8 shows the levels of the second and third harmonic products relative to the fundamental signal at the dummy load. It is noted that there is considerably more third harmonic than second, particularly at the lower frequency.

TABLE 8. MEASURED SECOND AND THIRD HARMONIC PRODUCTS OF THREE-MESH PAC OPERATING AT 5-KILOWATT PLATE POWER LEVEL

Operating Frequency f_0 (MHz)	Measured Harmonic Attenuation in dB	
	At $2f_0$	At $3f_0$
2.05	133	111.5
3.99	134.8	127.1

Note: Two PAC assemblies were tested at 2.05 MHz, the results being averaged above. Power output P_0 was approximately 3200 watts in all cases.

Additional harmonic measurements were made with the setup shown in figure 25. The 4CX5000A beam tetrode was operated in the same grounded-grid circuit with polarizing potentials of 7500 volts on the plate, 1250 volts on the screen, and -280 volts on the grid (as before), but a number of changes were made in the instrumentation and in the test procedure. The intermediate power amplifier (IPA) stage of the AN/FRT-39A and the AN/URC-32 radio set were used to study possible effects of different sources of excitation and, in some tests, a two-mesh bandpass transmitting filter was employed to insure a pure, sinusoidal driving signal. Figure 25 also shows a capacitive divider in place of the metalized resistor assembly at the dummy load and several changes, as compared with figure 24, regarding instrumentation in the screened room. The signal generator was used in these tests to establish relative harmonic levels at point "B." These data were transformed to the common load, point "A," from knowledge of the capacitive divider's attenuation which ranged from 23 to 26 dB at the frequencies of interest.

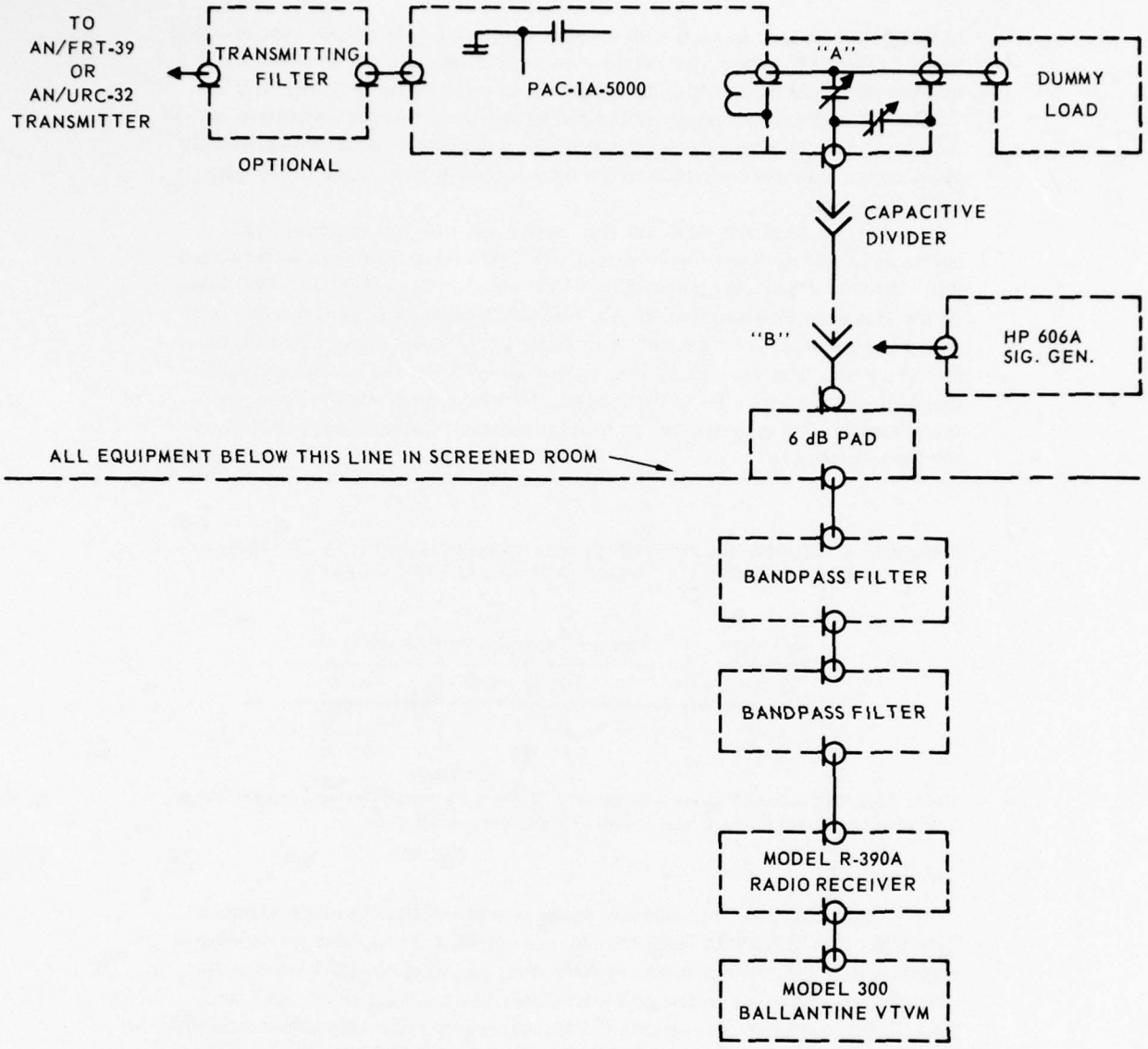

Figure 25. Block diagram of setup used in measuring levels of major harmonic signals from 5-kilowatt PAC assembly at 50-ohm dummy load.

Results of typical measurements for three different levels of output power P_0 in the dummy load are shown in table 9. These data at 2 MHz compare in a general sense with data in table 8 at 2.05 MHz when the same output power was supplied. If we make allowances for unavoidable experimental error, we find that the different test setups and procedures described in connection with figures 24 and 25 give similar results when measuring harmonics. The data in tables 8 and 9 lead to the following general observations:

1. The 4CX5000A beam tetrode gives appreciably more output at $3f_0$ than at $2f_0$ when operated under conditions employed in the AN/FRT-39A radio transmitter. (Note that the 3-400Z power triodes gave comparably low distortion products at all harmonics shown in table 6.)

2. As the driving power of the 4CX5000A tetrode is reduced, the second and third harmonics are reduced, in general, about the same as the fundamental output level.

3. The level of harmonic energy in the output clearly depends upon the purity of the excitation. This is shown by the improvement afforded by the auxiliary filter and indicated by the high level of the third harmonic when the AN/URC-32 transmitter was hard pressed to give enough drive for an output power of 3200 watts in the (c) part of table 9.

TABLE 9. MEASURED SECOND- AND THIRD-HARMONIC SIGNALS OF THREE-MESH PAC WITH 4CX5000A TUBE OPERATING AT DIFFERENT POWER LEVELS WITH DIFFERENT SOURCES OF EXCITATION

Sources of Excitation Operating at f_0 = 2 MHz	Measured Harmonic Attenuation in dB (P_0 denotes power in 50-ohm load in watts)					
	Second Harmonic (4 MHz)			Third Harmonic (6 MHz)		
	P_0 = 3200	P_0 = 1600	P_0 = 800	P_0 = 3200	P_0 = 1600	P_0 = 800
(a) IPA of AN/FRT-39A without filter	−134.5	−137.0	−141.0	−109.5	−111.0	−111.5
(b) IPA of AN/FRT-39A with auxiliary filter	−138.0	−142.0	−143.0	−110.5	−113.0	−116.0
(c) AN/URC-32 transmitter without filter	−135.5	−137.5	−140.0	−107.0	−115.0	−116.0

CROSS-MODULATION MEASUREMENTS

Cross-modulation is defined as modulation of a desired signal by an undesired signal.[5] This form of modulation (sometimes called intermodulation) occurs in a transmitting multicoupling system when one or more signals in the common load circuit are not sufficiently attenuated by the coupling networks, causing a form of high-level modulation at the plates of the power amplifier tubes.

The major cross-modulation products of two three-mesh PAC assemblies were measured using the instrumentation shown in figure 26. The IPA sections of two AN/FRT-39A transmitters were used as drivers in obtaining nominal plate power outputs of 4.9 and 3.6 on successive tests. This power reduction of some 1.3 dB was used with operating frequencies separated 2.5 and 5 percent in the vicinity of 2 and 4 MHz. Table 10 gives measured levels of third- and fifth-order cross-modulation products relative to the fundamental power levels at the 50-ohm load under the foregoing conditions.

The measuring technique was similar to the one used in measuring harmonics at high-power. Referring to figure 26, after the receiver and all three filters had been tuned to the frequency of each cross-modulation product, its level at point "B" was determined by means of the standard signal generator. The attenuation of the capacitive divider was added to give the level at the load, point "A."

The results in table 10 illustrate in a general way the levels of major cross-modulation products to be expected with these particular power tubes operating under the specified conditions with two three-mesh PAC assemblies and a standard dummy load. The data show that cross-modulation levels decrease with wider frequency separations and lower operating powers, as expected, but the scope of the study was too limited to warrant any conclusions regarding the cross-modulation levels that are realizable in a well-designed transmitting installation employing the PAC approach.

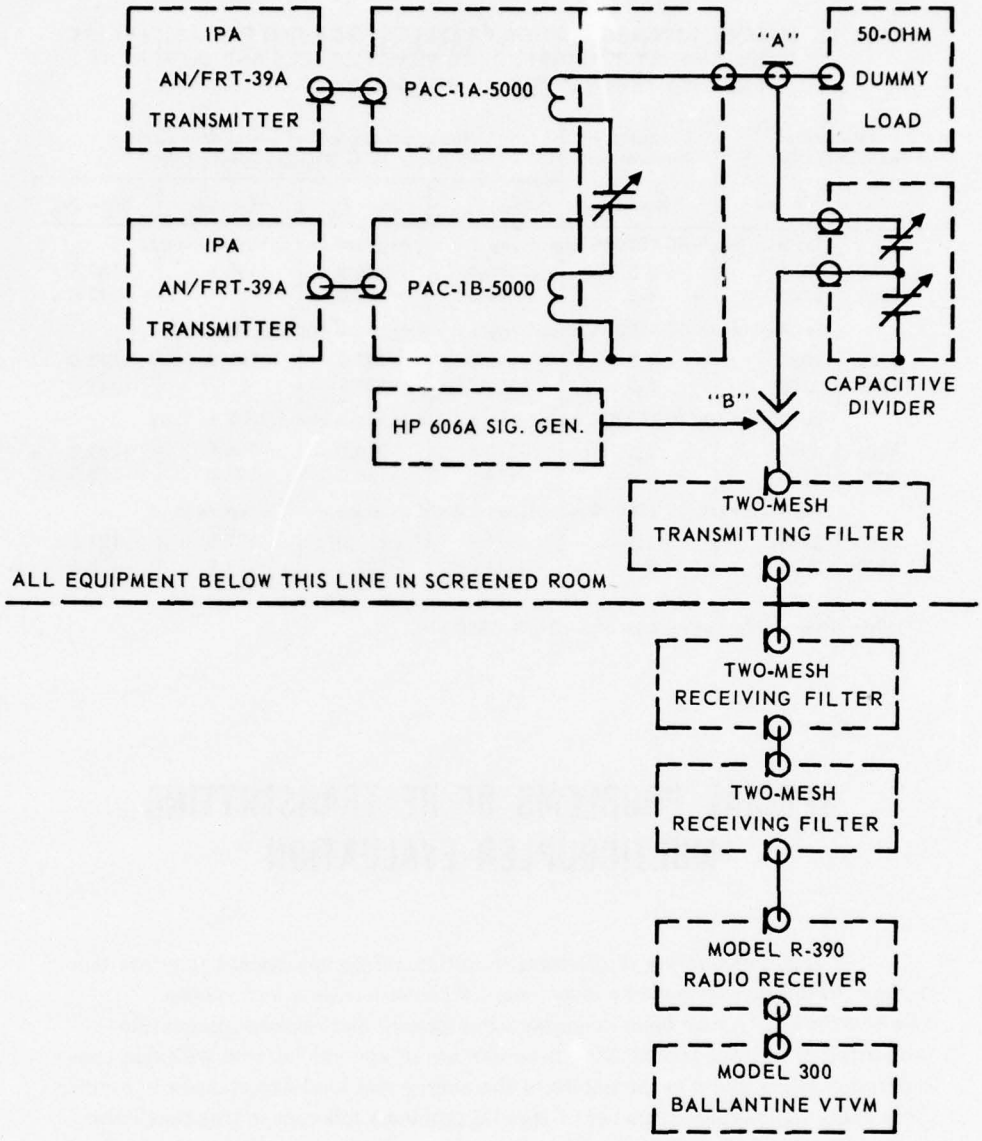

Figure 26. Block diagram of setup used in measuring major cross-modulation products with two PAC assemblies operating simultaneously into a 50-ohm dummy load.

TABLE 10. MAJOR CROSS-MODULATION PRODUCTS FROM TWO PAC ASSEMBLIES OPERATING AT TWO DIFFERENT POWER LEVELS AND DIFFERENT FREQUENCY SEPARATIONS WITH 50-OHM LOAD

Fundamental Frequencies (kHz)		Frequency Separation	Measured Levels of Cross-Modulation Relative to Fundamentals (dB)			
f_a	f_b	(percent)	$2f_a - f_b$	$2f_b - f_a$	$3f_a - 2f_b$	$3f_b - 2f_a$
(a) With each 4CX5000A supplying 4.9 kW at plate and 3.1 kW to load.						
2000	2050	2.5	−110.5	−106.5	−138.0	−137.5
2000	2100	5.0	−121.5	−123.5	(*)	−142.0
(b) With each 4CX5000A supplying 3.6 kW at plate and 2.3 kW to load.						
2000	2050	2.5	−112.0	−109.0	−142.0	−140.0
2000	2100	5.0	−123.5	−127.5	(*)	−141.0
(c) With each 4CX5000A supplying 4.9 kW at plate and 3.1 kW to load.						
4000	3900	2.5	−110.0	−116.0	−135.0	−135.5
4000	3800	5.0	−118.5	−120.0	−136.0	−138.0
(d) With each 4CX5000A supplying 3.6 kW at plate and 2.3 kW to load.						
4000	3900	2.5	−111.0	−117.0	−137.5	−137.0
4000	3800	5.0	−121.0	−122.0	−138.0	−138.5

(*) One filter would not tune to $3f_a - 2f_b = 1800$ kHz.

SPECIAL PROBLEMS OF HF TRANSMITTING MULTICOUPLER EVALUATION

A sound evaluation of alternative multicoupling approaches requires that a clear distinction be made between coupler characteristics and system characteristics. As we have seen, both the forward and reverse attenuation properties of passive transmitting networks are of special interest with due consideration being given to the nature of the source and load experienced in practice. This section pinpoints a number of special problems inherent in this particular evaluation effort, describes several alternative procedures available, and indicates the magnitude of some sources of error experienced in this limited test program.

It is important to understand the true nature of the alternative approaches under investigation. As illustrated in figure 27, the conventional approach includes several radio transmitters and couplers with a form of matching network that facilitates multiple operation with a common broadband antenna. The proposed PAC approach in figure 27B shows the power amplifier and coupling network integrated with a common distribution line. The immediate objective is to evaluate the relative merits of these alternative approaches and the present series of tests was prescribed for this purpose.

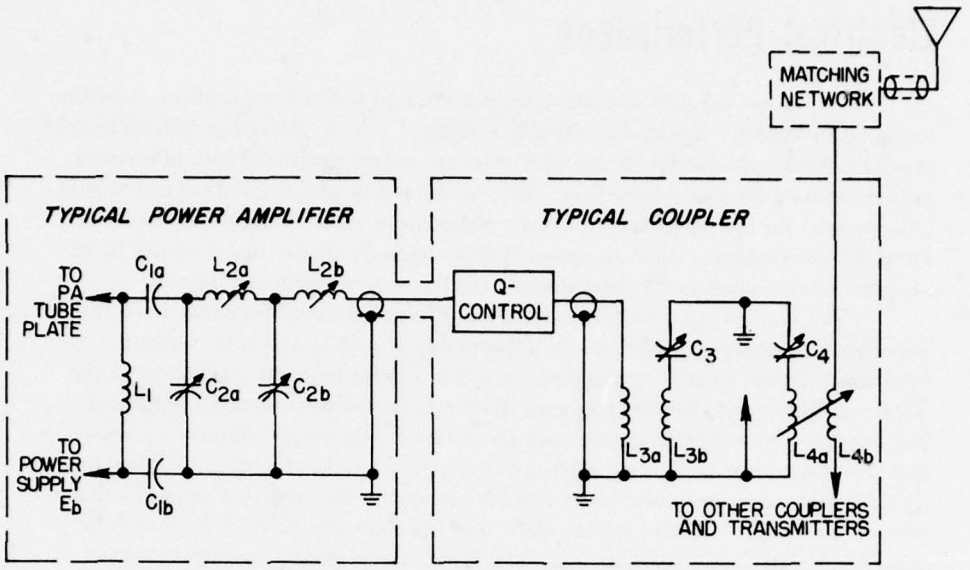

A. CONVENTIONAL SHIPBOARD TRANSMITTING MULTICOUPLER APPROACH

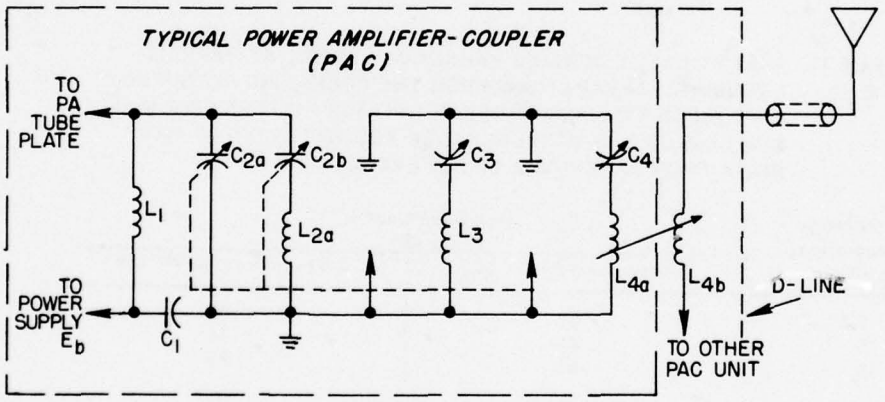

B. PROPOSED INTEGRATED APPROACH

Figure 27. The two alternative multicoupler approaches under consideration.

Electrical Performance

The electrical performance characteristics of typical transmitting couplers are specified today "in standard 50-ohm systems." As explained in MIL-STD-220A, insertion loss is measured by use of a standard signal generator with attenuator calibrated for a 50-ohm termination. This technique is straightforward and reasonably precise for the comparison of filter and coupler units designed for these standard terminations, but it is apparent from figure 27 that neither coupler is in any sense terminated in 50 ohms through the frequency bands of interest.

The present multicoupler evaluation affords an excellent example of the importance of analytical methods in network design. It is a simple matter to compare different coupler configurations under similar terminal conditions at the source and load and, for this purpose, idealized conditions are often indicated. For example, consider the question of the relative selectivity afforded by two- and three-resonator coupler assemblies that give the same midband insertion loss. By analytical means convenient charts for answering this question were developed several years ago.[6] These charts show that the three-resonator design affords considerably better selectivity than the two-resonator design having the same minimum midband loss and resonators with the same unloaded Q-factor (table 11). Moreover, temperature stability is improved by distributing the power dissipation (37 percent in this example) over three resonators rather than two of similar design.

TABLE 11. ANALYTICALLY DERIVED VALUES OF LOSS L_s AT VARIOUS FREQUENCY SEPARATIONS FROM THE OPERATING FREQUENCY f_0 AT WHICH TWO- AND THREE-RESONATOR FILTERS GIVE MINIMUM LOSS OF 2 dB WITH UNLOADED RESONATOR Q'S OF 1000 (DATA FROM APPENDIX A OF REFERENCE 5).

Frequency Separation (percent)	Stop-Band Loss L_s (in dB)	
	2 Resonators, Q_L = 200	3 Resonators, Q_L = 138
2.5	36	47
5	48	65
10	61	85

Physical Features

It is unnecessary to stress the importance of major physical differences in most cost and evaluation studies. The particular combination of equipments employed in the present tests reflect a number of unique physical characteristics that are not self-evident and lead to highly questionable comparisons if not properly considered. Reference is made to the fact that some of the couplers possess physical features that enable them to pass standard shock and vibration tests whereas other couplers do not.

In figure 27A, the particular coupler specified was the AN/SRA-35(V)(XN-2). While this equipment has been installed aboard a number of major communications ships, it was never intended to satisfy shock, vibration, and other environmental requirements of MIL-E-16400E. Questionable features include the variable vacuum capacitors with glass envelopes and the large, poorly supported helical inductors that comprise the main elements of the resonators. The PAC resonators would be properly identified as exploratory developmental models, as defined in MIL-STD-243A, and yet resonators of this general design have successfully passed shock and vibration requirements for shipboard electronic equipment of this type. Since a major objective of this hf resonator design is to provide the highest practicable unloaded Q, it is clear that dielectric materials in the form of coil supports and capacitor envelopes should be of high quality and kept to a practical minimum. In consequence, it is clearly unreasonable to make direct performance or cost comparisons between couplers that satisfy standard shipboard requirements and couplers that do not.

VARIOUS SOURCES OF NONLINEAR PRODUCTS

Tests prescribed in this limited evaluation included measurements of third- and fifth-order intermodulation or cross-modulation products as well as harmonic levels relative to fundamental energy in the common load. Thus, it is important to consider the various sources of nonlinear products that may significantly influence these measurements.

Low-Level Stages

With the high-power amplifier tubes operating in the so-called linear mode, any major nonlinear or other spurious products in the driving source can be expected to influence the unwanted products in the common load. Considerable difficulty was experienced during early tests when the AN/URC-32A was used to drive the 3-400Z's to 1 kilowatt output. As illustrated in figure 28, the waveform of the excitation used in tables 6 and 7 was monitored on a Tektronics Type 555 Dual-Beam Oscilloscope, and excitation was limited to avoid serious distortion products. An L-type matching network was used to provide a VSWR of 1:1 for the IPA of the AN/FRT-39A. This materially improved the excitation waveform of the 4CX5000A power triode in table 8 along with subsequent two-channel PAC tests. As noted earlier, however, the 4CX5000A beam tetrodes were *not* operated in the same circuit configuration employed in the AN/FRT-39A transmitter. The PAC circuit necessitated changes in the method of supplying high voltage to the plate of the 4CX5000A. Special plate chokes were fabricated and the feedback circuits were modified to avoid unstable operation at certain frequencies. (Time and effort have not been available to determine the effects of these changes on the operating characteristics of the power tubes.)

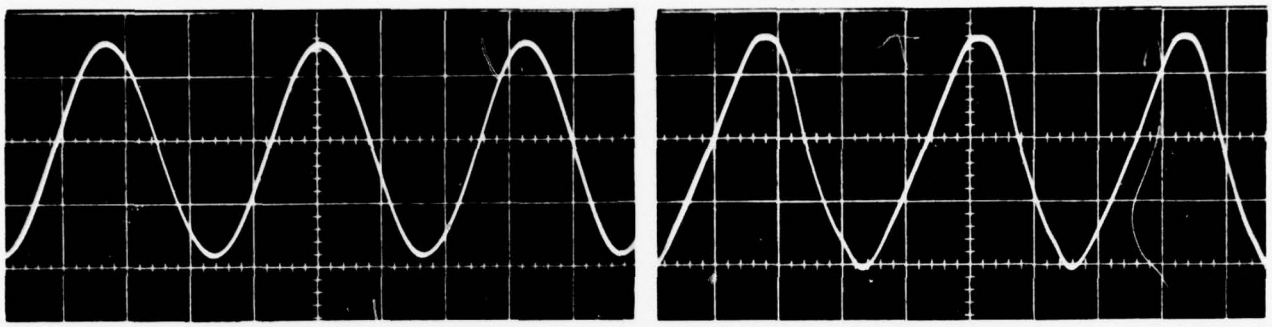

NO GRID CURRENT FULL POWER

A. OPERATING AT 2 MHZ

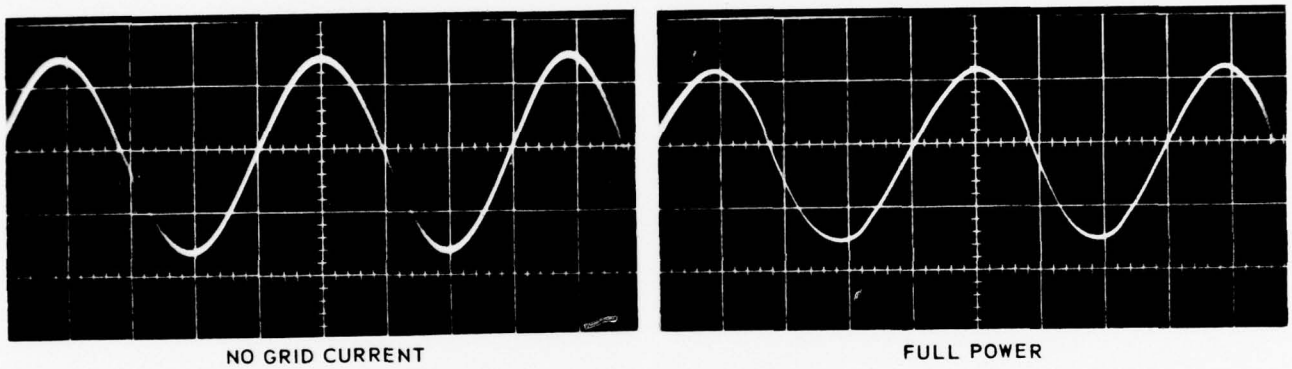

NO GRID CURRENT FULL POWER

B. OPERATING AT 4 MHZ

Figure 28. Oscillograms showing excitation waveforms with PAC operating at different power levels and at different frequencies.

Instrumentation and Indicators

Test instruments with nonlinear probes, such as vacuum tube voltmeters and reflectometers, can seriously influence the level of spurious energy in the common load. Consequently, probes of this type were removed when these energy levels were being measured.

Nonlinear Components

Resistors, inductors, and capacitors which exhibit a nonlinear relationship between rates of change of current and voltage are, of course, to be avoided.

Resistors utilizing a semiconducting material manifest both nonlinearity and current noise.[7] For this reason, metallized resistors and vacuum capacitors were used in fabricating the voltage dividers used in this study.

It is natural to expect some nonlinear response from inductors with ferromagnetic core material, particularly in high-power applications, and a special effort was made to avoid magnetic material whenever possible in constructing experimental PAC and D-line equipment. However, it is observed (fig. 4) that ferrite is used in the cathode choke of the 4CX5000A tube, and the AN/FRT-39A transmitter uses the same arrangement, along with adjustable iron cores in two inductors (*L*-912 and *L*-913) in the transmitter's output circuit. A few tests were conducted early in the test program to investigate possible intermodulation effects of these core materials. Odd-order products were compared on a spectrum analyzer as the output inductors with iron cores (connected in parallel) were replaced by a variable coil with the same inductance without any core. With the 3000-kHz carrier suppressed, two equal cw signals were employed at 2998 and 3002 kHz, respectively. There was no significant change in level of the third through ninth intermodulation products as equal inductance values, with and without iron cores, were substituted in the output circuit of the AN/FRT-39A. Later tests were conducted with and without the ferrite core material in the cathode choke and, as before, no significant changes in intermodulation levels were discernible.

Nonlinear Characteristics of Dummy Loads

Tests were conducted early in 1967 to select the most linear dummy load unit from a group of six different types that were available in the vicinity of the NELC Transmitter Laboratory. By measuring the level of third harmonic energy from PAC-1A-1000 operating at 4 MHz, for example, a special load consisting of 5500 feet of RG-17/U in tandem with 3000 feet of RG-8/U coaxial cable gave a value of –134 dB while the levels obtained from five dummy loads of commercial design were from 19 to 45 dB higher. This group of commercial 50-ohm loads included two different 500-watt units and an 18-kilowatt unit without special provisions for cooling, plus two high-power units cooled by water or oil. While these limited results must be considered tentative, they clearly indicate that certain commercial dummy loads can cause significant errors in measuring spurious signals from medium to high-power transmitting equipment.

Nonlinear Effects of Cable Fittings

The possibility of serious nonlinear effects from certain coaxial cable fittings was pinpointed by NEL-sponsored studies conducted aboard USS BUNKER HILL in 1966. These studies indicated that Type UG-30 D/U bulkhead feedthrough connectors caused the third harmonic component of a transmitter (supplying 800 watts to a 50-ohm dummy load near 8 MHz) to increase by 20 to 27 dB, depending upon the connector employed. The probable reason for this was given as the fact that "the connectors were partially made of steel."

With relatively high currents flowing through the connectors, it was concluded that "the steel was being driven hard enough to generate substantial third harmonic levels."[8] Since a UG-30 D/U feedthrough connector had been used for years to supply rf energy to the screened room in the NELC Transmitter Laboratory, a number of UG-30 D/U and UG-30 E/U connectors were obtained from Navy stock and tested using the instrumentation shown in figure 24. With the PAC-1A-1000 supplying 500 watts to the coaxial load at 4 MHz, no increase in the level of the third harmonic component was noted using either type of connector. Both the UG-30 D/U and the newer UG-30 E/U connectors utilize short lengths of magnetic material in their inner and outer conductor assemblies. Later, additional connectors of this type were tested at a higher power level. With the PAC supplying 2 kilowatts at 2.05 MHz into the coaxial load (terminated in a Jones Model 6322 500-watt dummy load unit), the level of second harmonic energy was measured using three samples of each of the following connector types: UG-29 B/U, UG-30 D/U, and UG-30 E/U. Moreover, after each connector was tested, data were recorded with the unit reversed. Except for two of the Type UG-30 E/U units, the level of second harmonic energy remained constant (within ±1 dB). Using two of the three UG-30 E/U connectors, the harmonic level dropped 9 to 11 dB as the orientation of the connector was reversed in the load circuit. The drop indicated that some harmonic generation was occurring, depending upon the effectiveness with which connections were made. This was confirmed when the harmonic level returned to normal after each connector was rotated and tightly secured in both of the mating UG-57 B/U fittings used with adapters to accommodate the RG-17/U cable in the load. These and other tests show the desirability of keeping unnecessary connectors out of the measuring installation and serve to emphasize the importance of secure, noncorroded contacts. However, these tests do not support the theory that the magnetic material used in Type UG-30 D/U feedthrough connectors is a significant source of harmonic energy at the frequencies and power levels employed in these studies.

Contact Resistance Effects

Apart from corroded or poorly fitting connectors, there are many other metal-to-metal contacts in a typical transmitting installation that can contribute to the nonlinear products in the common load. While all mechanical contacts are potential sources, special problems arise from relays, switches, and spring contacts in general, since their constriction resistance tends to be relatively large. The voltage-current characteristic of this resistance has been shown to be inherently nonlinear.[7] In consequence, mechanical connections are to be avoided wherever possible, particularly in high-power transmitting installations.

Power Amplifier Operating Characteristics

Tubes of the same type differ widely in their electrical characteristics, and even greater differences in linearity result when their associated circuits are not adjusted in a comparable manner. The magnitude of the problem is illustrated by wide variations in spurious signals measured as a function of load impedance using several communications transmitters.[9] This matter deserves special emphasis in evaluating those multicoupling installations in which the ancillary couplers are not adjusted to give a VSWR exactly equal to unity on the interconnecting lines to the transmitters. Assuming that the transmitters are initially tuned and loaded with a 50-ohm dummy load, it is clear that system performance is degraded as the load presented by the couplers departs from this value, depending upon the values of complex loads provided and the electrical lengths of the interconnecting lines.

Effects of Distribution System and Complex Antenna Loads

Direct comparison of the nonlinear products of different transmitting multicoupler installations is unrealistic unless comparable distribution techniques are utilized. All schemes now used in combining transmitting couplers are essentially low-loss passive LC networks and it is inevitable that they introduce certain reactance values in the common load circuit, considering the rather broad operating band. Reactance in the common load circuit necessitates compensating adjustments in the couplers' output meshes and this adversely affects the attenuation characteristics, particularly at small percentage frequency separations in the reverse direction. It follows, therefore, that the levels of nonlinear products in a practical working system will be higher, in general, than the levels measured in a two-channel (diplexing) setup with a 50-ohm resistive load.

PROBLEMS OF MEASURING SMALL SIGNALS

A summary of several power levels commonly used in transmitting multicoupler studies may be helpful in pinpointing several additional sources of measurement error and in appraising the relative effectiveness of the two alternative approaches under consideration.

The thermal noise power available from a matched generator of resistance R_g is

$$p_n = \frac{E_n^2}{4 R_g} = kTB \tag{8}$$

where E_n, the available noise voltage, is given by

$$E_n = \sqrt{4kTR_gB} \tag{9}$$

The remaining terms are:

k (Boltzman's constant) = 1.38×10^{-23} joule/degree
T (absolute temperature) = 273 + degrees centigrade

and

B = noise bandwidth in hertz

With $T = 293°$ Kelvin and $B = 3000$ hertz, the reference noise power is

$$p_n = kTB = 1.213 \times 10^{-17} \text{ watt} \tag{10}$$

This is about 210 dB below the power level of a 10 kW radio transmitter.

In communications system engineering, the power available from a receiving antenna to a matched 50-ohm receiver may be of interest. The level of received energy is sometimes compared with the signal required to give 1 microvolt at the receiver's input terminals. This requires an open-circuit voltage E_{oc} of 2 microvolts at the receiving antenna's terminals, the power available to the receiver being (neglecting line losses):

$$p_{avail} = \frac{E_{oc}^2}{4R_r} = \frac{4 \times 10^{-12}}{4 \times 50} = 2 \times 10^{-14} \text{ watt} \tag{11}$$

in the case of a matched 50-ohm receiver. This reference receiving power level is roughly 32 dB above kTB in equation (10) and 175 dB below the transmitting level of 5 kilowatts or so employed in many of the present tests.

In attempting to measure weak nonlinear products in the presence of these strong fundamental signals, the problem of providing adequate filtering for a sensitive measuring device has proved to be rather difficult. Because of the number of cross-modulation and harmonically related frequencies involved, suitable crystal filters were not available and only two two-mesh manually tuned receiving filters could be found for the range of frequencies of immediate interest. (The Center's supply of auxiliary filters of this type was recently exhausted in order to satisfy urgent shipboard requirements.) Two filters provided adequate attenuation for harmonic measurements (fig. 25) but had to be supplemented by another two-section transmitting filter for cross-modulation measurements (fig. 26). Table 12 gives the measured insertion loss of these two- and three-filter combinations at frequencies in the vicinity of 4 MHz. The table also shows different levels of third- and fifth-order cross-modulation products measured with comparable transmitting power levels using these filter combinations.

TABLE 12. MEASURED INSERTION LOSS OF TWO- AND THREE-FILTER COMBINATIONS IN FIGURES 25 AND 26 IN THE VICINITY OF THEIR OPERATING FREQUENCIES NEAR 4 MHz, WITH EFFECTS OF THESE FILTER COMBINATIONS ON MEASURED CROSS-MODULATION LEVELS

A. Insertion loss measured in 50-ohm system

f/f_a (f_a = 4 MHz)	Measured Insertion Loss (dB)		Difference in Measured Loss
	Two Filters	Three Filters	
0.950	70.0	109.5	39.5
0.975	51.0	78.0	27.0
1.000	17.0	18.0	1.0
1.025	42.0	66.0	24.0
1.050	54.0	90.0	36.0

B. Comparison of cross-modulation levels measured using two and three filters (relative to 1 microvolt across 50-ohm dummy load)

Cross-Modulation Product	Test Frequency (kHz)	Measured Level (dB)		Measurement Difference (dB)
		Two Filters	Three Filters	
(a) With 2.5 percent spacing (f_b/f_a = 0.975)				
$2f_a-f_b$	4100	55.5	37.0	18.5
$2f_b-f_a$	3800	55.5	30.0	25.5
$3f_a-2f_b$	4200	24.5	12.0	12.5
$3f_b-2f_a$	3700	29.0	12.5	16.5
(b) With 5 percent spacing (f_b/f_a = 0.950)				
$2f_a-f_b$	4200	38.0	28.0	10.0
$2f_b-f_a$	3600	44.5	30.0	14.5
$3f_a-2f_b$	4400	21.0	12.5	8.5
$3f_b-2f_a$	3400	21.5	10.0	11.5

BASIC CRITERIA FOR EVALUATING HF TRANSMITTING MULTICOUPLERS

A sound evaluation of alternative multicoupling approaches must include a large number of important considerations not included in this limited test program. A separate study of the essential cost and effectiveness aspects of this matter has been reported[10] and it is unnecessary to undertake a complete review of these various factors at this time. The present discussion is concerned with criteria that are believed to be essential for a sound technical appraisal of any hf transmitting multicoupling system.

Shipboard Interference Must Be Substantially Reduced

The recent Exercise BASE LINE II showed that serious problems of communications interference are widespread throughout the Fleet. This is especially true aboard ships having major command and control responsibilities such as AGMR and CC classes which are expected to receive weak signals in proximity to a large number of high-power hf transmitters. The magnitude and seriousness of this problem must not be underestimated, and causes of this interference must be identified to facilitate corrective action. In view of the level of interference normally experienced aboard ship from rusty bolt and other environmental effects, are existing hf transmitter and two-mesh coupler designs adequate for most future needs? As we shall see, this study adds to a growing body of analytical and empirical evidence that substantially better equipment designs and installation practices are needed.[1,3]

The chart in figure 29 illustrates major facets of this problem. In addition to typical ambient noise levels experienced aboard ships and the amount of isolation commonly realized between hf transmitting and receiving antennas, levels of third-order cross-modulation products measured in the present test program are indicated in relation to kTB. The level of environment or "hull generated" interference aboard a relatively clean ship is also indicated (62 dB above kTB), based on recent tests performed aboard USS BUNKER HILL by IIT Research Institute.[10]

In figure 29, the *lower limits* of the cross-hatched areas denote average values of third-order cross-modulation products measured with the conventional transmitter-multicoupler arrangement, using frequency separations of 2.5 and 5 percent. These average levels may be compared with the levels obtained with two three-mesh PAC assemblies operating at the same frequency spacings and fundamental power levels (approximately 205 dB above kTB). The levels of third-order products from the PAC assemblies are seen to be 20 and 26 dB below the corresponding average levels from the conventional installation. Note that both installations give average spurious signals that are appreciably above the level expected from a clean shipboard environment.

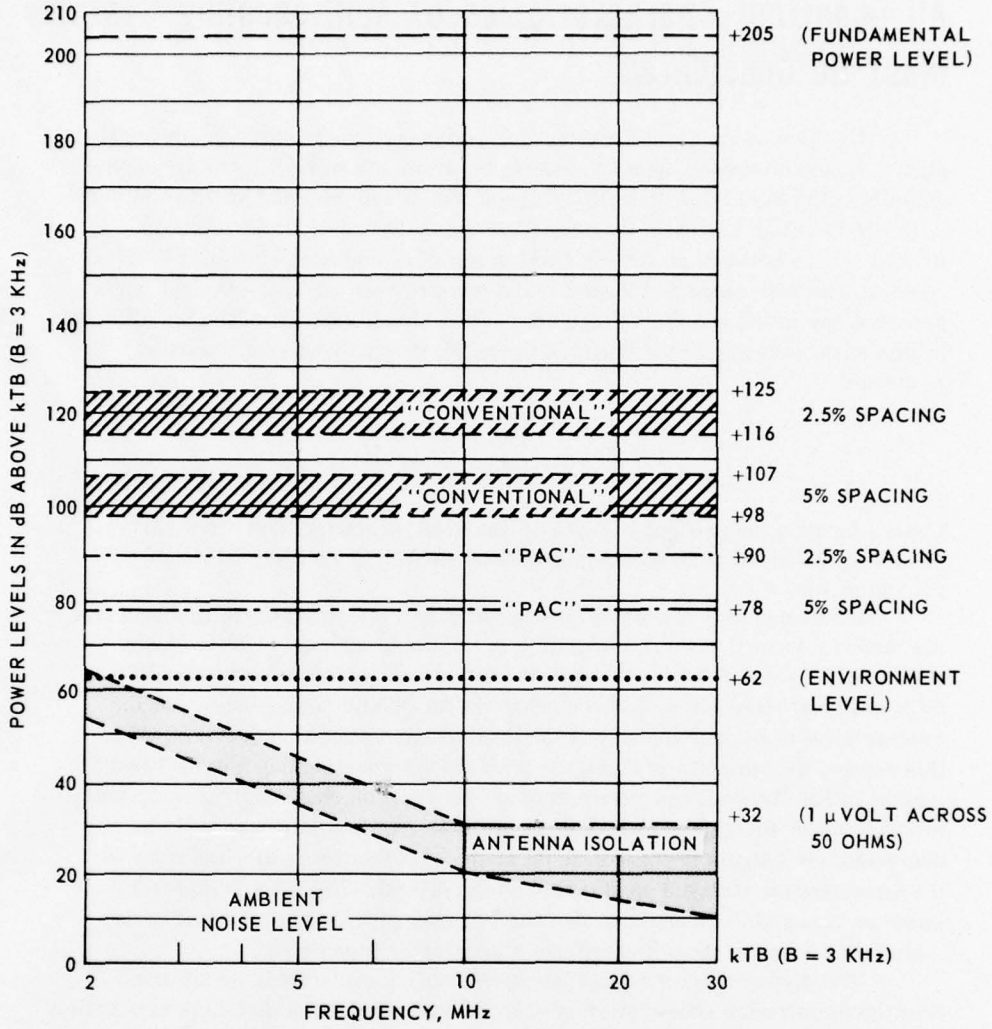

Figure 29. Measured levels of third-order cross-modulation products from conventional installation of AN/FRT-39A transmitters and AN/SRA-35 diplexer and from three-mesh PAC assemblies under comparable conditions. Effects of four different lengths of interconnecting lines are shown by cross-hatching and antenna isolation commonly realized aboard ship is shown by shading.

All Important Characteristics of Multicoupling Systems Must Be Considered

By eliminating several components and operations required in conventional practices, the integrated approach affords important advantages by removing undesirable effects of interconnecting lines on the attenuation and VSWR characteristics of operating systems. As shown in figures 30 and 31, three arbitrary lengths of line between an AN/FRT-39A transmitter and an AN/SRA-35(V)(XN-2) coupler, with both tuned and loaded in the recommended manner, introduce major perturbations in the reverse voltage attenuation characteristics of the installation. In this case, referring to the insert in figure 29, reverse voltage attenuation is defined

$$\alpha_r = 20 \log_{10} \left| \frac{E_s}{E_r} \right| \quad \text{(log units)}$$

Depending upon the particular length of line used, secondary nulls in these curves are observed at frequency separations extending well beyond the 10 percent points.

It is especially important to note that major effects of these line sections are largely obscured when consideration is limited to average results. Along with a succession of displaced nulls, the different lines often give increased attenuation at frequencies above or below the null point. In consequence, the average level of attenuation across the band remains somewhat constant. For this reason, the variation in measured third-order products using four different lengths of line between the "conventional" transmitting and coupling equipment is indicated by the cross-hatched areas in figure 29. No effort was made to determine line lengths that gave maximum cross-modulation levels and many of the measurements changed appreciably as the AN/SRA-35(V)(XN-2) diplexer was jarred or "banged." Because of the small number of tests performed, it is unrealistic to consider these line effects statistically unimportant.

The performance of a practical multicoupling system may be different from the performance characteristics of individual couplers or diplexing assemblies. A meaningful evaluation should include a representative number of transmitting circuits operating at full power with a complete combining or distribution scheme and with loads that accurately simulate complex antenna impedances commonly experienced. Under these conditions, interference predictions will be of real value in shipboard communication system engineering.

Above all, consideration should be given to operating characteristics of the system. Reliable performance cannot be achieved if operations are complicated by excessive interaction and are subject to wide variations. The importance of design simplicity is emphasized both for reliability and economy in automatic control, and for speed and convenience in manual operations.

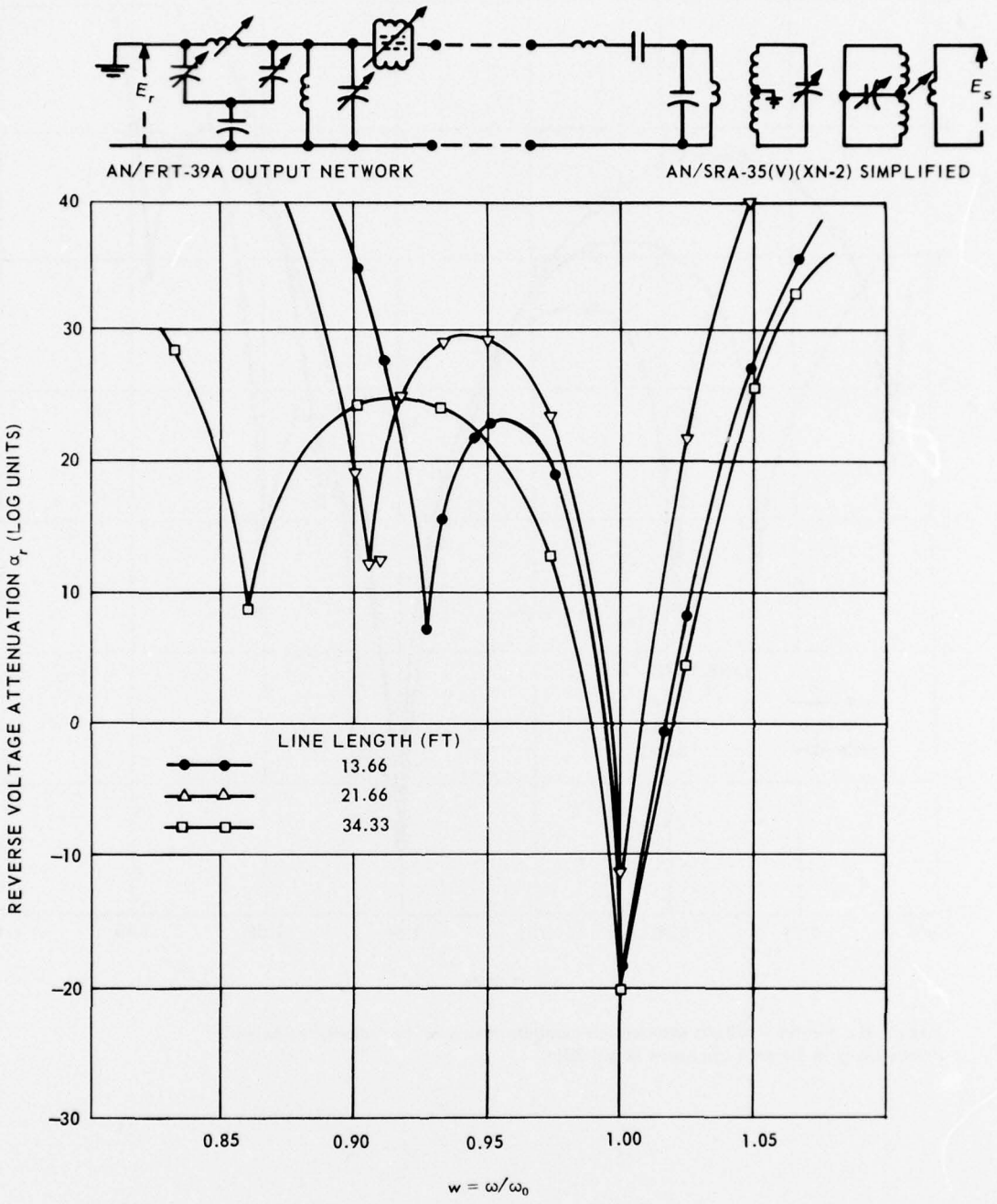

Figure 30. Reverse voltage attenuation characteristics of AN/FRT-39A and AN/SRA-35 (V)(XN-2) measured at 2.4 MHz using different lengths of interconnecting cable.

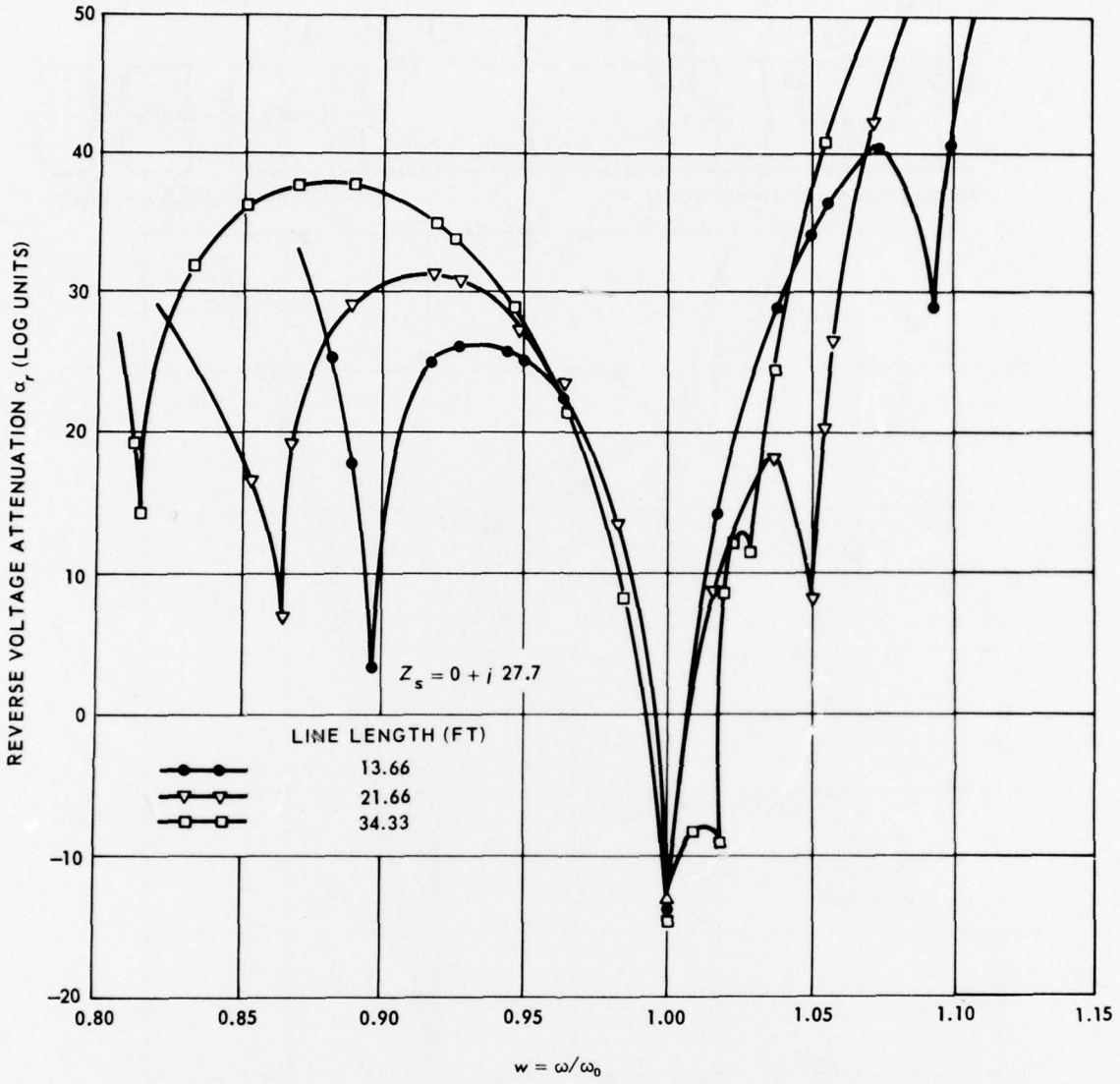

Figure 31. Reverse voltage attenuation characteristics of the transmitter-coupler combination in figure 5 measured at 5.4 MHz.

OTHER FACTORS TO BE CONSIDERED

In planning advanced communications systems to satisfy future requirements, several broad questions arise that are not directly connected with equipment tests. Several general considerations having an important bearing on the present work will be briefly discussed.

Changes in Naval Communications Are Inevitable

No blanket criticism of current procurements of manually tuned ancillary multicouplers is implied by efforts to develop truly advanced automatic equipments to satisfy future needs. It is self-evident, however, that problems and deficiencies inherent in present-day equipment designs and installation practices must be identified and appraised objectively if progress is to be made in naval communications system engineering.

Major Problems Must Be Attacked Simultaneously

Owing to the long lead time inherent in military equipment development, the Navy cannot afford to postpone advanced multicoupler system development while the search continues for means to alleviate serious problems in the shipboard environment. It must be assumed that progress will be made in eliminating or reducing rusty bolt effects and other long-standing problems inherent in traditional methods of designing and fabricating elements of ships' superstructure. Accordingly, advanced equipment designs and specifications should not be predicted upon the pessimistic view that little progress can be expected in related problem areas.

Obsolete Equipment Must Be Replaced

With the advent of satellite communications, a growing tendency to downgrade the importance of high-frequency problems has become apparent. There is no evidence that the Defense Department plans to abandon its extensive high-frequency communications capabilities in the foreseeable future, and there is strong evidence that much of the communications equipment in the Fleet is obsolete and will have to be replaced soon. The present stockpile of hf multicouplers is practically depleted. It follows that additional multicoupler procurements are inevitable in the next few years and, if advanced designs are to be available when needed, the long cycle of development, procurement, and evaluation must proceed without further delay.

Related Applications Must Be Considered From the Outset

The importance of commonality has only recently received the emphasis it deserves in military planning. While the present discussion has been arbitrarily limited to the shipboard hf transmitting multicoupler problem, the approach was planned from the outset to apply to comparable hf receiving problems and to a wide variety of transmitting and receiving applications at uhf and at the higher frequencies employed by communications satellites. Also, it is self-evident that automatically controlled, integrated transmitting and receiving multicouplers are applicable to a variety of land-based, underwater, and airborne applications of several branches of the military.

CONCLUSIONS

While the following conclusions are based primarily on this limited empirical study of integrated power amplifier-coupler equipment, certain comparisons are made with results obtained with a conventional installation of AN/FRT-39A radio transmitters and an AN/SRA-35(V)(XN-2) diplexer.*

1. Compared with conventional two-mesh coupler installations, the three-mesh PAC reduces the average levels of third-order cross-modulation around 20 dB with 5 percent frequency spacing and about 26 dB with 2.5 percent spacing.

2. When effects of four arbitrary lengths of interconnecting lines are considered with the conventional installation, the PAC gives improvements in third-order cross-modulation levels of as much as 29 dB with 5 percent frequency separation and as much as 35 dB with 2.5 percent separation.

3. These substantial reductions in cross-modulation levels are obtained using a passive three-mesh network whose passband efficiency equals or exceeds that of the two-mesh coupler and transmitter combination.

4. No significant difficulties were experienced operating either the PAC or the conventional equipment for extended periods at full power. However, problems of mechanical instability were noted in testing the AN/SRA-35(V)(XN-2) diplexer.

5. The PAC and conventional installations attenuate major harmonic radiation products in a comparable manner.

---

*Results of tests on the conventional installation furnished by another NELC group.

RECOMMENDATIONS

1. Procure sufficient service test models of power amplifier-coupler (PAC) and bandpass distribution line (D-line) equipment to facilitate a full-scale testing and evaluation program in a simulated shipboard installation.

2. In the meantime, perform analyses and tests to more completely delineate the capabilities and limitations of the modular bandpass D-line. This investigation should include the use of two complementary D-lines with a common antenna load (both real and simulated).

3. Extend the integrated PAC concept to radio receiving systems.

4. Conduct studies to facilitate the integration of transmitting and receiving couplers with a common antenna.

5. Perform analytical and empirical studies to permit realistic predictions of cross-modulation products generated in representative power amplifier tubes, taking into account forward and reverse characteristics of PAC equipment.

REFERENCES

1. Navy Electronics Laboratory Report 1279, *Predesign of High-Power HF Transmitting Multicoupler System for SOUTHERN CROSS,* by S. E. Parker, p.13-50, 30 March 1965

2. Dishal, M., "Alignment and Adjustment of Synchronously Tuned Multiple-Resonant-Circuit Filters," *Institute of Radio Engineers. Proceedings,* v.39, p.1448-1455, November 1951

3. Navy Electronics Laboratory Report 1311, *HF Transmitter Couplers Compared With Integrated Power Amplifier-Couplers by Computer Analysis,* p.10-11, by S. E. Parker, 5 October 1965

4. Chaffee, E. L., "A Simplified Harmonic Analysis," *Review of Scientific Instruments,* v.7, p.384-389, October 1936

5. *The International Dictionary of Physics and Electronics,* Van Nostrand, 1956

6. Stanford Research Institute Contract AF 19(604)-2247; Final Report, *Design Data for Antenna-Multicoupler Systems,* by J. F. Cline and others, p.48-49, September 1959

7. Whitley, J. H., "Measuring Contact Constriction Resistance in Terms of Its Non-Linearity," *Electronic Instrument Digest,* v.4, p.7-11, July 1967

8. IIT Research Institute Report 56062-13, *Engineering Study for Electrical Hull Interaction,* by R. Elsner and others, p.14, 3 January - 1 August 1966

9. Electromagnetic Compatibility Analysis Center Technical Note TN-005-56, *Communication Transmitter Spurious Levels as a Function of Load Impedance,* by Z. S. Borowik, August 1966 (Also related report: Pan American World Airways Special Investigation Report 503-1-A, *Effect of Terminating Load on Transmitter Output Gross Effects, Phase 1A HF,* December 1964)

10. Naval Electronics Laboratory Center Report 1537, *Cost Effectiveness Comparison of Two Multicoupling Approaches to HF Transmitting System Engineering,* by S. E. Parker, 20 February 1968

UNCLASSIFIED

Security Classification

DOCUMENT CONTROL DATA - R & D

(Security classification of title, body of abstract and indexing annotation must be entered when the overall report is classified)

1. ORIGINATING ACTIVITY (Corporate author)
NAVAL ELECTRONICS LABORATORY CENTER
San Diego, California 92152

2a. REPORT SECURITY CLASSIFICATION
UNCLASSIFIED

2b. GROUP

3. REPORT TITLE
SOME ELECTRICAL AND OPERATING CHARACTERISTICS OF INTEGRATED POWER AMPLIFIER COUPLER EQUIPMENT

4. DESCRIPTIVE NOTES (Type of report and inclusive dates)
Research and Development Report, January-September 1967

5. AUTHOR(S) (First name, middle initial, last name)
S. E. Parker, J. M. Devan, W. J. E. Edwards, and L. G. Robbins

6. REPORT DATE
18 March 1968

7a. TOTAL NO. OF PAGES
64

7b. NO. OF REFS
10

8a. CONTRACT OR GRANT NO.

b. PROJECT NO. S32-78
Task 7398
(NELC J543)

c.

d.

9a. ORIGINATOR'S REPORT NUMBER(S)
NELC-1551

9b. OTHER REPORT NO(S) (Any other numbers that may be assigned this report)

10. DISTRIBUTION STATEMENT
This document is subject to special export controls and each transmittal to foreign governments or foreign nationals may be made only with prior approval of the Naval Electronics Laboratory Center.

11. SUPPLEMENTARY NOTES

12. SPONSORING MILITARY ACTIVITY
Naval Ship Systems Command
Department of the Navy

13. ABSTRACT

High-power hf power amplifier coupler (PAC) equipment was empirically evaluated to expedite an objective comparison with conventional multicoupling techniques. Results showed that (1) the performance of the PAC equipment is substantially in accordance with theoretical predictions; (2) the integrated three-mesh assembly provides greater selectivity than a conventional transmitter with a two-mesh coupler; (3) the present experimental PAC equipment is stable at the 10 kW (PEP) plate-power level.

DD FORM 1 NOV 65 1473 (PAGE 1)
S/N 0101-807-6801

UNCLASSIFIED
Security Classification

403 940

14. KEY WORDS	LINK A		LINK B		LINK C	
	ROLE	WT	ROLE	WT	ROLE	WT
Couplers - Performance						
Power amplifiers - Couplers						

CHIEF OF NAVAL MATERIAL
DNL 5
COMMANDER, NAVAL SHIP SYSTEMS COMMAND
SHIPS 035
SHIPS 00V
SHIPS 2052 (2)
SHIPS 204113
COMMANDER, NAVAL AIR SYSTEMS COMMAND
AIR 533E
AIR 5330
AIR 5336
AIR 604
COMMANDER, NAVAL ORDNANCE SYSTEMS COMMAND
ORD 0322
ORD 083
ORD 9132
COMMANDER, NAVAL ELECTRONIC SYSTEMS COMMAND
ELEX 913
COMMANDER, NAVAL SHIP ENGINEERING CENTER
CODE 6170
CODE 6175B
CODE 6175.02
CODE 6178
CODE 6179B
CODE 6179C03
CODE 6179C07
NAVAL SHIP ENGINEERING CENTER
SAN DIEGO DIVISION
CHIEF OF NAVAL PERSONNEL
PERS 11B
PERS A3
CHIEF OF NAVAL OPERATIONS
OP-03EG
OP-311
OP-312F
OP-345
OP-506G
OP-07T
OP-71
OP-713
OP-724
OP-098S
OP-922Y4C1
OP-94G
CHIEF OF NAVAL RESEARCH
CODE 418
CODE 427
CODE 437
CODE 454
CODE 455
CODE 458
CODE 461
CODE 466
CODE 468
COMMANDER IN CHIEF
US PACIFIC FLEET
CODE 93
US ATLANTIC FLEET
COMMANDER OPERATIONAL TEST AND EVALUATION FORCE
COMMANDER, KEY WEST TEST & EVALUATION DETACHMENT
DEPUTY COMMANDER OPERATIONAL TEST AND EVALUATION FORCE, PACIFIC
COMMANDER CRUISER-DESTROYER FORCE
US PACIFIC FLEET
CODE 425
US ATLANTIC FLEET
COMMANDER SUBMARINE FORCE
US PACIFIC FLEET
COMMANDER ANTISUBMARINE WARFARE FORCE
US PACIFIC FLEET
US ATLANTIC FLEET
COMMANDER FIRST FLEET
COMMANDER SECOND FLEET
COMMANDER TRAINING COMMAND
US ATLANTIC FLEET
COMMANDER AMPHIBIOUS FORCE, US PACIFIC FLEET
COMMANDER SERVICE FORCE, US ATLANTIC FLEET
COMMANDER, DESTROYER DEVELOPMENT GROUP, PACIFIC
COMMANDER FLEET AIR WINGS, ATLANTIC FLEET
NAVAL AIR DEVELOPMENT CENTER
LIBRARY
AVIATION MEDICAL ACCELERATION LABORATORY
NAVAL MISSILE CENTER
TECHNICAL LIBRARY
CODE N3232
NAVAL AIR TEST CENTER
NANEP
WEAPONS SYSTEMS TEST DIVISION
NAVAL WEAPONS CENTER
CHINA LAKE
CODE 753
CORONA LABORATORIES
TECHNICAL LIBRARY
NAVAL UNDERSEA WARFARE CENTER
LIBRARY
FLEET COMPUTER PROGRAMMING CENTER
PACIFIC
LIBRARY
ATLANTIC
TECHNICAL LIBRARY
NAVAL WEAPONS LABORATORY
LIBRARY
PEARL HARBOR NAVAL SHIPYARD
CODE 246P
PORTSMOUTH NAVAL SHIPYARD
CODE 242L
SAN FRANCISCO BAY NAVAL SHIPYARD
PHILADELPHIA NAVAL SHIPYARD
CODE 249C
CHARLESTON NAVAL SHIPYARD
CODE 240
NAVAL SHIP RESEARCH & DEVELOPMENT CENTER
CARDEROCK DIVISION
APPLIED MATHEMATICS LABORATORY
CODE 860
LIBRARY
ANNAPOLIS DIVISION
CODE 257
NAVY MINE DEFENSE LABORATORY
CODE 716
NAVAL TRAINING DEVICE CENTER
TECHNICAL LIBRARY
CODE 02 (2)
NAVY UNDERWATER SOUND LABORATORY
LIBRARY
CODE 905
NAVAL AIR ENGINEERING CENTER
AEROSPACE CREW EQUIPMENT LABORATORY
LIFE SCIENCES RESEARCH GROUP
NAVAL CIVIL ENGINEERING LABORATORY
L54
NAVAL RESEARCH LABORATORY
CODE 2027
CODE 4320
CODE 5250
CODE 5320
CODE 5400
CODE 5440
NAVAL ORDNANCE LABORATORY
WHITE OAK
DIVISION 730
DIVISION 880
BEACH JUMPER UNIT ONE
BEACH JUMPER UNIT TWO
FLEET ASW SCHOOL
TACTICAL LIBRARY
FLEET SONAR SCHOOL
NAVY MEDICAL FIELD RESEARCH LABRATORY
LIBRARY
NAVAL UNDERWATER WEAPONS RESEARCH AND ENGINEERING STATION
LIBRARY
OFFICE OF NAVAL RESEARCH BRANCH OFFICE
PASADENA
CHIEF SCIENTIST
BOSTON
LONDON
NAVAL TRAINING CENTER
SERVICE SCHOOL COMMAND
TRAINING DEPARTMENT
NAVAL SCHOOL OF AVIATION MEDICINE
CODE 31
NAVAL SHIP MISSILE SYSTEMS ENGINEERING STATION
CODE 903
ELECTRONICS MAINTENANCE ENGINEERING CENTER
CODE 1923
NAVAL PERSONNEL RESEARCH ACTIVITY
SAN DIEGO
NAVAL OCEANOGRAPHIC OFFICE
CODE 1640
SUPERVISOR OF SHIPBUILDING, CONVERSION & REPAIR, US NAVY
GROTON, CONN.
CODE 249
NAVAL POSTGRADUATE SCHOOL
LIBRARY
NAVAL APPLIED SCIENCE LABORATORY
CODE 222
CODE 920
NAVAL ACADEMY
ASSISTANT SECRETARY OF THE NAVY (RESEARCH AND DEVELOPMENT)
NAVAL SCIENTIFIC AND TECHNICAL INTELLIGENCE CENTER (IE)
NAVAL SECURITY GROUP
G43
COMMANDANT OF THE MARINE CORPS
OFFICE OF THE DEPUTY CHIEF OF STAFF
RESEARCH AND DEVELOPMENT
SUBMARINE FLOTILLA ONE, US PACIFIC FLEET
DEFENSE DOCUMENTATION CENTER (20)
DEPARTMENT OF DEFENSE RESEARCH AND ENGINEERING
TECHNICAL LIBRARY
WEAPONS SYSTEMS EVALUATION GROUP
DEFENSE ATOMIC SUPPORT AGENCY
DOCUMENT LIBRARY SECTION
FEDERAL AVIATION AGENCY
SYSTEMS RESEARCH AND DEVELOPMENT SERVICE
MILITARY COORDINATION (RD-52.1)
NATIONAL OCEANOGRAPHIC DATA CENTER
CODE 2400
NATIONAL ACADEMY OF SCIENCES/ NATIONAL RESEARCH COUNCIL
COMMITTEE ON UNDERSEA WARFARE
ARCTIC RESEARCH LABORATORY
FEDERAL COMMUNICATIONS COMMISSION
OFFICE OF THE CHIEF ENGINEER
CENTRAL INTELLIGENCE AGENCY
OCR/DD-STANDARD DIST.
NATIONAL SECURITY AGENCY
P-224
R-31
DEFENSE COMMUNICATIONS AGENCY
COMMUNICATIONS SATELLITE PROJECT OFFICE
NATIONAL BUREAU OF STANDARDS
BOULDER, COLO.
VETERANS ADMINISTRATION CENTER
AUDIOLOGY-SPEECH PATHOLOGY CLINIC
NATIONAL LIBRARY OF MEDICINE
BUREAU OF COMMERCIAL FISHERIES
LA JOLLA, CALIF.
TUNA RESOURCES LABORATORY LA JOLLA
WOODS HOLE, MASS.
BIOLOGICAL LABORATORY LIBRARY
ELECTROMAGNETIC COMPATIBILITY ANALYSIS CENTER
NAVENGRXSTA
NAFEC LIBRARY
ARMY MATERIAL COMMAND
AMCRD-DE-E-S
ASST CHIEF OF STAFF FOR INTELLIGENCE, US ARMY
SYSTEMS DEVELOPMENT DIVISION
ARMY MEDICAL RESEARCH AND DEVELOPMENT COMMAND
MEDDH-SR
ABERDEEN PROVING GROUND
ARMY HUMAN ENGINEERING LABORATORIES
TECHNICAL LIBRARY
ARMY TEST AND EVALUATION COMMAND
HDQTRS AMSTE-EL
ARMY RESEARCH AND DEVELOPMENT ACTIVITY
ELECTRONIC WARFARE DIVISION
ELECTRONIC DEPARTMENT
ARMY MISSILE COMMAND
REDSTONE SCIENTIFIC INFORMATION CENTER
DOCUMENT SECTION
ARMY ELECTRONICS RESEARCH AND DEVELOPMENT LABORATORY
ARMY ELECTRONICS COMMAND
ELECTRONIC WARFARE LABORATORY
AMSEL-WL-D
MANAGEMENT & ADMINISTRATIVE SERVICES DEPT
AMSEL-RD-MAT
INSTITUTE FOR EXPLORATORY RESEARCH
AMSEL-XL-C
HARRY DIAMOND LABORATORIES
LIBRARY
FRANKFORD ARSENAL
HUMAN FACTORS LABORATORY
SMUFA N6400/202-4
PICATINNY ARSENAL
TECHNICAL INFORMATION BRANCH
SMUPA-VA6
ARMY RESEARCH OFFICE (DURHAM)
CRD-AA-IP
WHITE SANDS MISSILE RANGE
STEWS-ID-E
HUMRRO DIVISION NO. 2 (ARMOR)
LIBRARIAN
ARMY ELECTRONIC WARFARE LABORATORY
MOUNTAIN VIEW OFFICE
OAKLAND ARMY BASE
COMMUNICATIONS DIVISION
WA-MTMTS (ELECTRONICS BRANCH)
ARMY AIR DEFENSE BOARD
SUPPORT DIVISION
FORT HUACHUCA
52D USASASOC
ARMY ENGINEER RESEARCH AND DEVELOPMENT LABORATORIES
TECHNICAL DOCUMENT CENTER
AIR FORCE HEADQUARTERS
DIRECTOR OF COMMAND CONTROL & COMMUNICATIONS
AFOCCBC
AIR DEFENSE COMMAND
ADOOA
AIR UNIVERSITY LIBRARY
AUL3T-5028
STRATEGIC AIR COMMAND
OAST
AIR FORCE EASTERN TEST RANGE
AFMTC TECHNICAL LIBRARY - MU-135
ROME AIR DEVELOPMENT CENTER
EMLAL-1 (DOCUMENT LIBRARY)
AIR PROVING GROUND CENTER
PGBPS-12
1ST STRATEGIC AEROSPACE DIVISION
DCI
AIR FORCE SCHOOL OF AEROSPACE MEDICINE
AEROMEDICAL LIBRARY
WRIGHT-PATTERSON AIR FORCE BASE
AIR FORCE SECURITY SERVICE
ESD/ESG
ELECTRONICS SYSTEMS DIVISION
ESTI
UNIVERSITY OF MICHIGAN
OFFICE OF RESEARCH ADMINISTRATION
NORTH CAMPUS
COOLEY ELECTRONICS LABORATORY
RADAR AND OPTICS LABORATORY
THE RADIATION LABORATORY
UNIVERSITY OF CALIFORNIA-BERKELEY
ELECTRONICS RESEARCH LABORATORY
UNIVERSITY OF CALIFORNIA-SAN DIEGO
MARINE PHYSICAL LABORATORY
MICHIGAN STATE UNIVERSITY
LIBRARY-DOCUMENTS DEPARTMENT
COLUMBIA UNIVERSITY
ELECTRONIC RESEARCH LABORATORIES
DARTMOUTH COLLEGE
RADIOPHYSICS LABORATORY
CALIFORNIA INSTITUTE OF TECHNOLOGY
JET PROPULSION LABORATORY
CORNELL UNIVERSITY
LIBRARY, CENTER FOR RADIOPHYSICS AND SPACE RESEARCH
HARVARD COLLEGE OBSERVATORY
HARVARD UNIVERSITY
GORDON MCKAY LIBRARY
LYMAN LABORATORY
LEHIGH UNIVERSITY
DEPARTMENT OF PSYCHOLOGY
GEORGIA INSTITUTE OF TECHNOLOGY
ENGINEERING EXPERIMENT STATION
ELECTRONICS DIVISION
UNIVERSITY OF WASHINGTON
APPLIED PHYSICS LABORATORY
TUFTS UNIVERSITY
INSTITUTE FOR PSYCHOLOGICAL RESEARCH
OHIO STATE UNIVERSITY
ANTENNA LABORATORY
UNIVERSITY OF HAWAII
ELECTRICAL ENGINEERING DEPARTMENT
THE UNIVERSITY OF TEXAS
DEFENSE RESEARCH LABORATORY
STANFORD UNIVERSITY
STANFORD ELECTRONICS LABORATORIES
DOCUMENTS LIBRARY
STANFORD RESEARCH INSTITUTE
NAVAL WARFARE RESEARCH CENTER
MASSACHUSETTS INSTITUTE OF TECHNOLOGY
RESEARCH LABORATORY OF TECHNOLOGY
DOCUMENT ROOM
ENGINEERING LIBRARY
LINCOLN LABORATORY
LIBRARY, A-082
RADIO PHYSICS DIVISION
THE JOHNS HOPKINS UNIVERSITY
APPLIED PHYSICS LABORATORY
DOCUMENT LIBRARY
INSTITUTE FOR DEFENSE ANALYSES
DOCUMENT LIBRARY